universität wien

MASTERARBEIT / MASTER'S THESIS

Titel der Masterarbeit / Title of the Master's Thesis

"Abundance and activity of marine bacteria, specifically *Alteromonas*, in the waters off West Greenland"

verfasst von / submitted by

Helena Cvetkovic

angestrebter akademischer Grad / in partial fulfilment of the requirements for the degree of

Master of Science (MSc)

Wien, 2024 / Vienna 2024

Studienkennzahl lt. Studienblatt / degree programme code as it appears on the student record sheet:	UA 066 833
Studienrichtung lt. Studienblatt / degree programme as it appears on the student record sheet:	Masterstudium Ecology in Ecosystems
Betreut von / Supervisor:	Univ.-Prof. Dr. Gerhard J. Herndl

Acknowledgements

First of all, I would like to thank myself for being persistent while working on the thesis, even though sometimes it seemed like it will never end. This is the biggest project I have done so far and, albeit with a lot of questioning of my own knowledge and motivation, I learned how rewarding it is to get results from your own work and that there is nothing more important to do than science, in terms of jobs of course. Therefore, I cannot wait for my scientific path to continue.

I want to thank Gerhard J. Herndl, my supervisor, for always being in a mood to discuss my results, guide me and give me honest critique. I´ve met him more than three years ago and his undying passion for learning and sharing knowledge is more than inspiring to us, students.

Special thank-you goes to Chie Amano, my co-supervisor, whose patience, laboratory and computational expertise made completion of this thesis possible. While there are people like Chie is, science is in good hands.

Lastly, I am grateful and privileged to have friends and family who have and will continue to support me in my quest to understand this world a little bit better.

Abstract

The Arctic Ocean is the oceanic region currently most affected by the global climate change. Consequently, the retreat of the Arctic Sea ice and the general warming of the Arctic waters might lead to major changes in the biota and ecosystems functioning of the Arctic Ocean. One of the most important drivers of the biogeochemical cycles in the marine environment are microbes. We followed the dynamics of the marine heterotrophic and autotrophic microbial community in the waters off West Greenland, specifically *Alteromonas*. Specific emphasis has been put on the contribution of *Alteromonas* on anaplerotic metabolism, i.e., the utilization of dissolved inorganic carbon (DIC) for biomass production. Using microautoradiography combined with catalyzed reporter deposition-fluorescence *in situ* hybridization (MICRO-CARD-FISH) we have determined the abundance, heterotrophic and chemolithoautotrophic or anaplerotic activity of the prokaryotes and *Alter-omonas* in the summer season in the waters off the coast of West Greenland. We found a depth-related distribution of *Alteromonas* with high abundances in the photic zone and a higher abundance at nearshore than offshore stations. Furthermore, the highest heterotrophic to chemolithoauto-trophic ratio was found in the photic zone, while the lowest ratio (< 1) was recorded for the bottom waters. *Alteromonas* was found to contribute 7.4 % to total prokaryotic DIC fixation and 4.4 % to prokaryotic heterotrophic activity. Thus, we conclude that *Alteromonas* could play a major role in the hetero- as well as autotrophic carbon cycling in the Arctic Ocean.

Keywords: West Greenland, MICRO-CARD-FISH, Alteromonas, DIC fixation

Contents

Table of Contents

Introduction

The Arctic

The melting of sea ice in polar regions is a widely recognised consequence of a global climate system changes (Kumar et al., 2010). Every year, the Greenland ice sheet loss is on average 281 gigatons of mass (https://gracefo.jpl.nasa.gov/resources/33/greenland-ice-loss-2002-2016/). The substantial influx of meltwater into oceanic systems results in the modification of physical and chemical properties of the Arctic Ocean. In addition to sea level rise, increased stratification and changes in the flow of oceans' currents represent the most important modified physical characteristics of the Arctic. This leads to changes in nutrient supply and exchange between deeper waters and the surface waters due to increased stratification (Padmasini et al., 2021). Even though there are reports of increased net primary production linked to the sea ice loss, it is still unknown how the nutrient flux to the surface waters affects primary production of this area (IPCC, 2019).

The coastal regions serve as interface between the land and marine environment. The marine system off the western coast of Greenland comprises Baffin Bay in the north, Davis Strait and the Labrador Sea in the south (Rysgaard et al., 2020). Within this region, two significant currents are observed: cold and fresh southward-flowing Baffin Island Current (BIC) and a warm and saline northward-flowing West Greenland Current (WGC) (Nansen, 1912).

The Arctic Ocean exhibits pronounced seasonality primarily influenced by sunlight (Leu et al., 2015). In winter, when the ice cover is complete, brine leakage contributes to vertical water mixing, bringing nutrients to the surface. At the beginning of the spring, the intensifying solar radiation accelerates the ice melt. The combination of favourable light conditions and nutrient availability fosters phytoplankton blooms. In this region, primary production occurs from April to September (Wassmann, 2011). With the diminishing solar radiation at the onset of au-tumn, the ice begins to form again. In the summer season, Nielsen and Hansen (1999) documented the presence of subsurface phytoplankton blooms situated near the pycnocline in Disko Bay, off the western coast of Greenland, particularly when the water column exhibited strong stratification. The authors also noted elevated bacterial abundance in the vicinity of the pycnocline, and the combined effects of these bacterial communities and the phytoplankton bloom potentially contribute to the overall productivity of the region (Nielsen and Hansen, 1999).

Microbial activity in the dark ocean

As sunlight penetrates down to 200 m depth, it leaves a significant fraction of the oceans' volume, approximately 1.27×10^{18} m^3 (Orcutt et al., 2011), in the dark, which represents the largest habitable region on Earth. The average abundance of prokaryotes in the deep oceanic water (bellow 200 m) is approximately 5×10^4 cells/mL corresponding to about 6.5×10^{28} cells (Whitman et al., 1998).

Microbes are active in the dark ocean albeit the organic matter decreases in its bioavailability with depth (Herndl et al., 2023). The occurrence and type of redox reactions depend on the availability of electron donors and acceptors, which further depends on horizontal and vertical mixing of water (Orcutt et al., 2011).

Heterotrophy, the utilization of organic carbon, was regarded as dominant metabolic path-way among prokaryotes in the dark ocean until a discrepancy between particulate organic carbon flux (POC) and heterotrophic prokaryotic carbon demand was observed (Baltar et al., 2009). This discovery has paved the way for the exploration of dissolved inorganic carbon (DIC) fixation, as

chemolithoautotrophy was found to contribute to the prokaryotic carbon demand as much as the POC flux (Baltar et al., 2010). The energy source for the dark DIC fixation might be reduced inorganic substances such as sulfur oxidation (Swan et al., 2011) However, there is also a possibility of anaplerotic metabolism of otherwise heterotrophic prokaryotes (Fig. 1).

Genus Alteromonas

The genus *Alteromonas* currently comprises eleven Gram-negative, heterotrophic bacterial species inhibiting marine, oxygen-rich environments (Ivanova et al., 2014). Widely recognized as r-strategists (allocating resources into reproduction as a mean of survival), these copiotrophs rapidly grow in the presence of nutrients utilizing complex macromolecules such as high molecular weight organic matter (Sherwood et al., 2016). Predominantly found in surface waters (Wolfer, 2023) and being r-strategists, it is not surprising that *Alteromonas* is not as common in polar as it is in tem-perate regions, although they are observed even in the deep ocean (Lopez-Lopez et al., 2005; Amano et al., 2022). Furthermore, it has recently been confirmed that *Alteromonas* can assimilate inorganic carbon in a process coined anaplerosis (Guerrero-Feijoo et al., 2017). First proof of heterotrophic bacteria fixing DIC was presented by Werkman and Wood (1942), and anaplerosis has since then been found in essentially all living heterotrophic organisms. Anaplerosis is a metabolic pathway responsible for replenishing intermediates within the citric acid cycle (TCA) (Topisirovic et al., 2016). There are several different anaplerotic reactions, but the one which occurs in prokaryotes is the carboxylation (reaction carried out in the presence of carbon dioxide as a substrate) of phos-phoenolpyruvate (PEP) to oxaloacetate (Fig. 1).

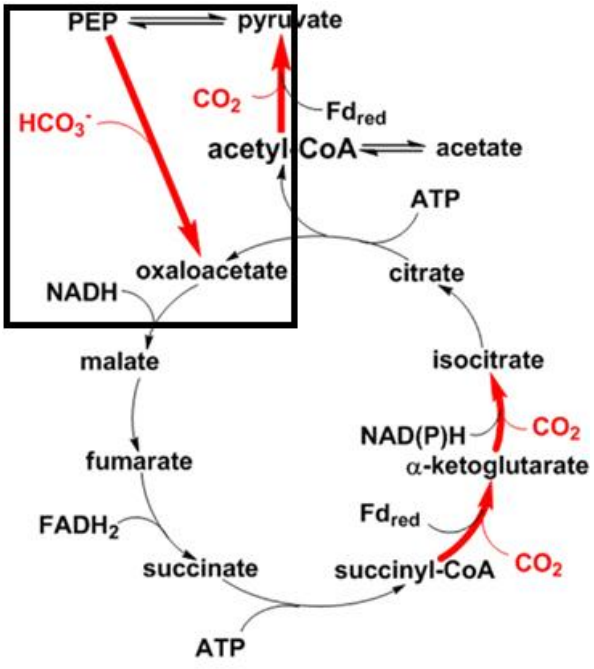

Figure 1. Citric acid cycle. Carboxylation of PEP to oxaloacetate (anaplerosis) is catalysed by PEP-carboxylase. Source: https://www.researchgate.net/figure/Autotrophic-CO2-fixation-pathways-in-phototrophic-organisms-The-CO2-assimilation-steps_fig4_51594568

Research questions

This study reports on the abundance and distribution of prokaryotes, as well as their heterotrophic and chemolithoautotrophic/anaplerotic activity, with a focus on *Alteromonas*. Our first research question is the relationship between heterotrophic and chemolithoautotrophic/anaplerotic activity of bacteria in this region, while the second is the rate of DIC fixation by *Alteromonas.* We

hypothesize that the importance of anaplerotic metabolism covaries with heterotrophic activity in marine *Alteromonas.*

Finding answers to these questions, we gain a deeper understanding of the system's functioning, principles of microbe distribution and their activity in this area.

Materials and Methods

Study site and sampling area

Water samples were collected along the western coast of Greenland (Fig. 2) during the ECOTIP project abroad RV *Dana* in July 2021. Seawater samples were collected from 13 stations using Niskin bottles mounted on a CTD (conductivity, temperature, depth) rosette system. Sampling locations were distributed over 5 transects, each of them comprising stations of the same latitude (Fig. 3). At each station, samples were taken at three different depths: surface (3 – 4 m), deep chlorophyll maximum (DCM) and near bottom (max. depth 678 m). Bulk activity of heterotrophic and autotrophic prokaryotes was determined by radioisotope tracer methods using ^{3}H-leucine and ^{14}C-bicarbonate, respectively (Reinthaler et al. 2010). Additionally, the abundance and single cell activity were determined by microscopy-based method with the selected samples from stations 8, 10, 17, 21, 24, 26, 28 and 30 (transects 2, 4 and 5).

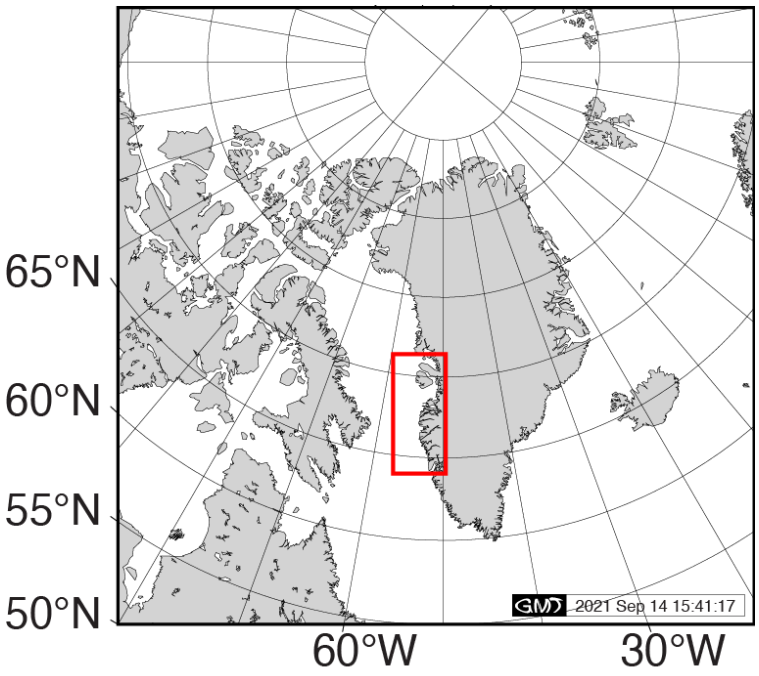

Figure 2. Map of Greenland. The sampling area is framed in red.

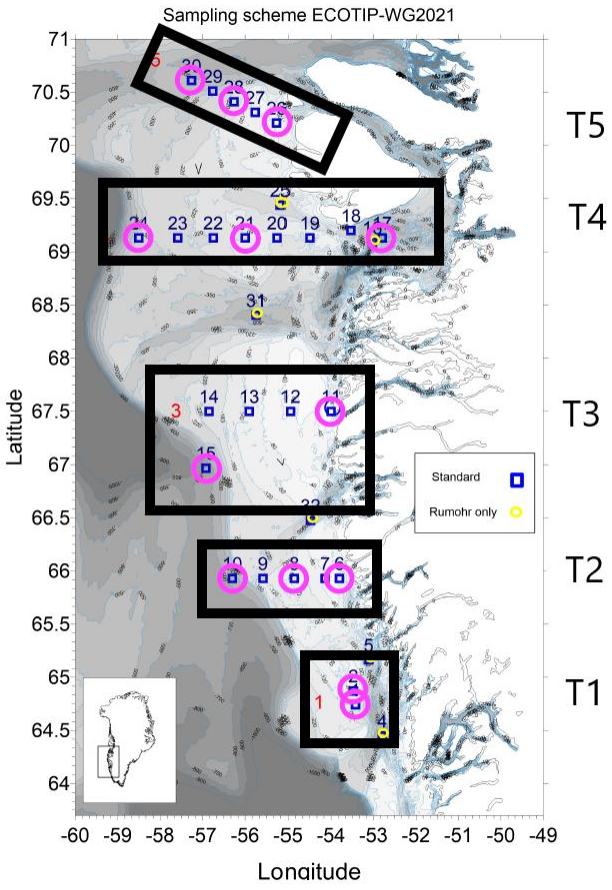

Figure 3. Transects sampled in this study (Transect 2, 3, 4 and 5 [T2, T3, T4, T5]). Each transect is comprising sampling locations (stations) at the same latitude.

Incubation and bulk leucine incorporation and dark DIC fixation

On the research vessel, 10 – 20 mL of seawater was incubated with either ^{3}H-leucine or ^{14}C-bicarbonate for 4.7 - 12.8 h and 48.4 - 72 h, respectively. The incubation was carried out in the cold room at approximately 5°C in the dark. After the incubation period, samples were fixed with 37 % formaldehyde to obtain a final concentration of 2 %. For ^{3}H-leucine incorporation measurements, filtration of fixed samples was carried out using 0.2 µm polycarbonate filters, followed by rinsing with MilliQ water. The filters samples were stored at – 20 °C until further analysis. For DIC fixation measurements, following the filtration step, the filters were fumed over concentrated HCl for 4 h to remove inorganic carbon from the filters.

For bulk leucine incorporation and dark DIC fixation measurements (Reinthaler et al. 2010), the filters were placed in 20 mL scintillation vials and 8 mL scintillation cocktail (Filter count, PerkinElmer) added. Subsequently, disintegration per minutes (DPM), were measured with a liquid scintillation counter (Tri-Carb 4910TR, PerkinElmer) in the home laboratory at the University Biology Building. The DPMs were converted to leucine incorporation rates.

CARD-FISH

Alteromonas abundance was determined by catalyzed reporter deposition-fluorescence *in situ* hybridization method (CARD-FISH) following the protocol of Herndl´s lab (2018). Samples were embedded with 0.1 % agarose and later permeabilized using 10 mL of permeabilization mixture (lysozyme, final concentration 10 mg/mL) at 37°C for 1 h. Before the hybridization, filters were cut to 1/12 of their original size. Following fluorescent oligonucleotide probes were used: Alt1413 (5´-TTT GCA TCC CAC TCC CAT-3´) to target *Alteromonas*, EUB338 I (5´-GCT GCC TCC CGT AGG AGT-3´) as positive control for hybridization and NON338 (5´-ACT CCT ACG GGA GGC AGC-3´) as a negative control. An aliquot of 299 µL of hybridization buffer containing 55 % formamide was mixed with 1 µL of a DNA probe at the concentration of 50 ng/µL. To prevent warming, probes were kept on the ice. Hybridization was carried out in the dark at 35°C for 15 h. Immediately after the hybridization, filters were washed in a prewarmed washing buffer (13 mM NaCl, 5 mM EDTA, 20 mM Tris-HCl, 0.01 % SDS) at 37°C for 15 min. Subsequently, 493 µL of the amplification buffer was mixed with 5 µL of Alexa 488 Tyramide (1 mg/mL green fluorescence). Samples were transferred in the mixture and incubated in the dark at 46°C for 15 min. After the amplification, filters were washed in 25 mL of PBS buffer mixed with Triton X-100 (final concentration 0.05 %) and rinsed three times with Milli-Q water. Before being air dried, filters were shortly dipped in 96 % ethanol. Before microautoradiography, a part of the filters was examined under the microscope to see if the hybridization worked properly. If the samples were accurately prepared, they were stored at - 20°C until further analyses.

Microautoradiography

Prokaryotic single-cell activity was determined by microautoradiography combined with CARD-FISH (Teira et al., 2004). Slide glasses were coated with prewarmed photographic emulsion (ILFORD, Nuclear emulsion) and placed on a cooled bench for 5 min. Samples were placed on the slide glasses and stored in black boxes with silica gel as a drying agent. Exposure time for the ^{3}H-leucine inoculated samples was 14 days, while for the ^{14}C-bicarbonate ones 30 days at 4°C. After exposure time ended, samples were developed and fixed at 17°C by placing slide glasses in developer solution (50 mL IFORD PHENISOL Developer and 200 mL Milli-Q) for 4 min, then washed in Milli-Q for 10 sec and placed in fixer solution (50 mL IFORD HYPAM Fixer and 200 mL Milli-Q) for 6 min. Final washing in Milli-Q was for 5 min. All steps were performed in a dark room in complete darkness due to the light sensitivity of the emulsion. After air drying, filters were counter-stained with ´4´,6-diamidino-2-phenylindole (DAPI, 2 µg/mL) and stored at – 20°C.

Samples were examined under Axio Imager M2 Carl Zeiss epifluorescence microscope. Three channels were used: DAPI (for all prokaryotes), FITC (for CARD-FISH positive cells, that is *Alteromonas*) and transmission light (for silver grains around active cells). A maximum of 12 photos (of different fields of views) of each sample with overlaying all three channels were taken with a digital camera mounted on the microscope. At least 1000 DAPI-stained cells were recorded per sample. The photos were analysed in AxioVision SE64 Re4.9 (Carl Zeiss) with an image analysis macro established by Zeiss.

Single-cell activity

The size of the silver grain area around active cells in µm^2 were converted to pmol of leucine and DIC substrate uptake per litre per h by relating the sum of the silver grain area of a sample to bulk leucine incorporation and bulk DIC fixation (Sintes and Herndl, 2006). The slope generated by the regression line (Fig. 4 and 5) was used to calculate conversion factor. Activity of each cell

was calculated using the equation: the single-cell activity [pmol/cell/h] = cell area [µm^2] / conversion factor / incubation time [h].

As for visual expression, number and width of bins of bar plots was decided using Sturge's formula (Sturge, 1926).

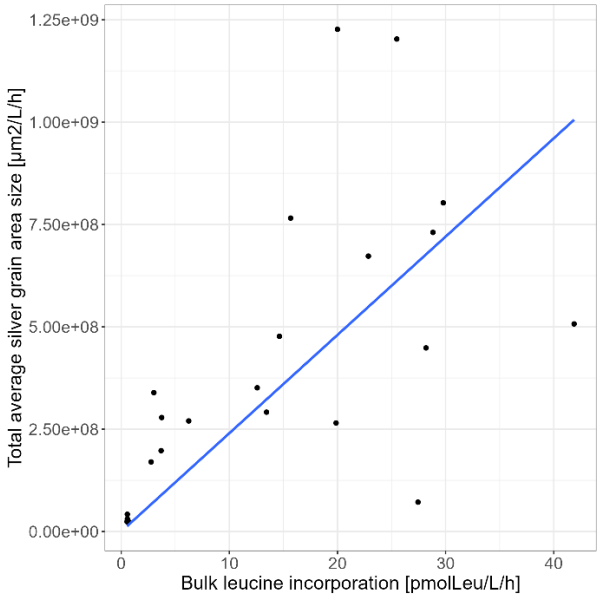

Figure 4. Relationship of the total silver grain area size [µm^2/L/h] per each sample inoculated with ^{3}H-leucine and bulk leucine incorporation [pmol/cell/h], R^2=0.7.

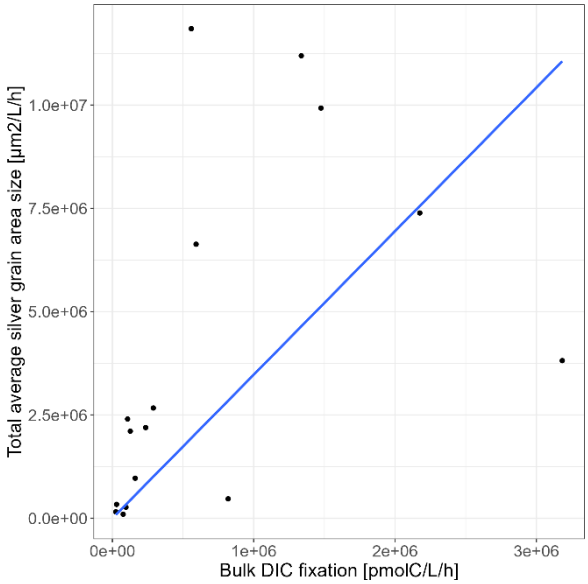

Figure 5. Relationship of the total silver grain area size [µm^2/L/h] per each sample inoculated with ^{14}C-bicarbonate and bulk DIC fixation [pmol/cell/h], R^2=0.49.

Bacterial abundance

Bacterial abundance was determined as cells stained with DAPI. At least 10 photos per sample were taken by overlapping DAPI and FITC channels, using a digital camera mounted on epifluorescence microscope. To count the cells from the photos an automated cell counting and enumeration software (ACMEtool3, https://www.mpi-bremen.de/en/automated-microscopy.html#section19794) was used.

Data analyses

Data analyses and visualization were performed in Excel (Microsoft Office 2021), R (version 4.3.1) (R Core Team, 2022, version 4.3.1), and Ocean Data View (version 5.6.7.). Packages used in R were: tidyr, dplyr, ggplot2, magrittr and reshape2.

Results

Physico-chemical characteristic of the water column

Temperature

Throughout the water column of all transects, temperature ranged from - 1.6 to + 6.6°C. Highest temperature was usually observed in the surface waters decreasing with depth, as shown in transect 1 (Fig. 6a). Higher temperatures were also recorded at nearshore then offshore stations (transect 2 - 4).

a) transect 1

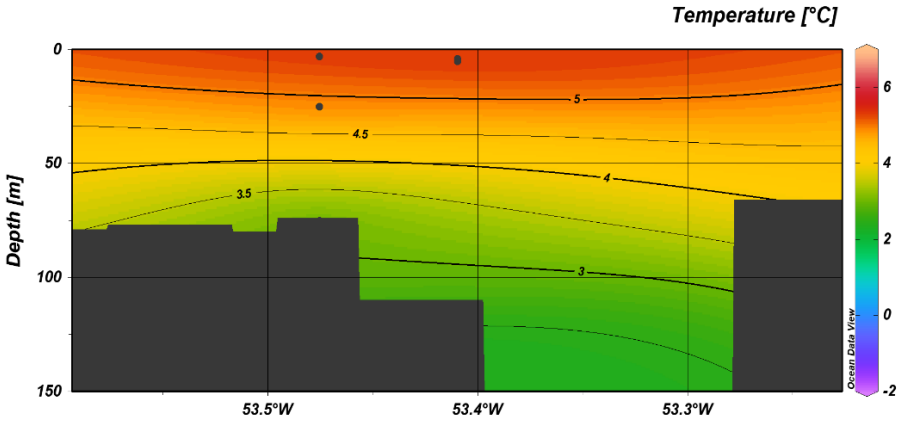

b) transect 2

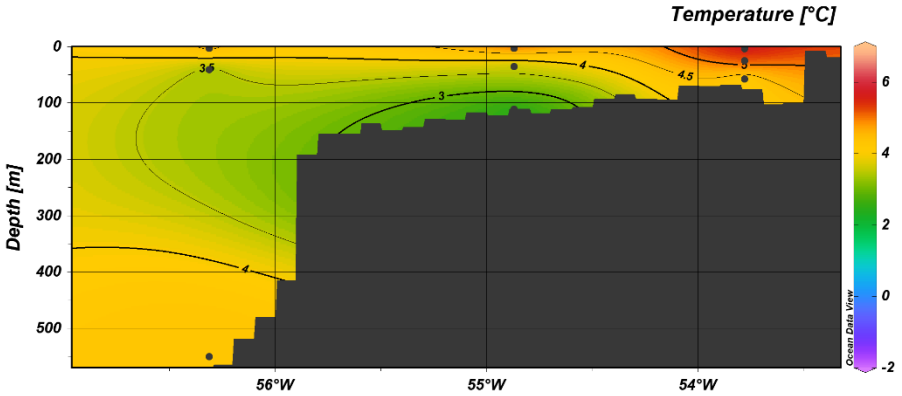

c) transect 3

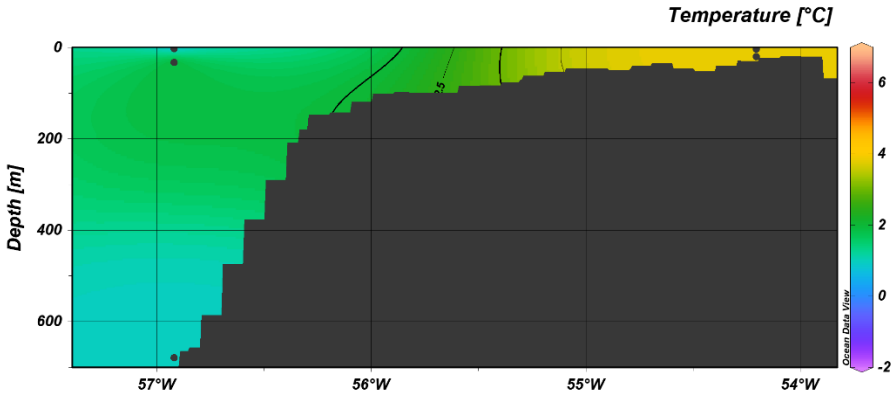

d) transect 4

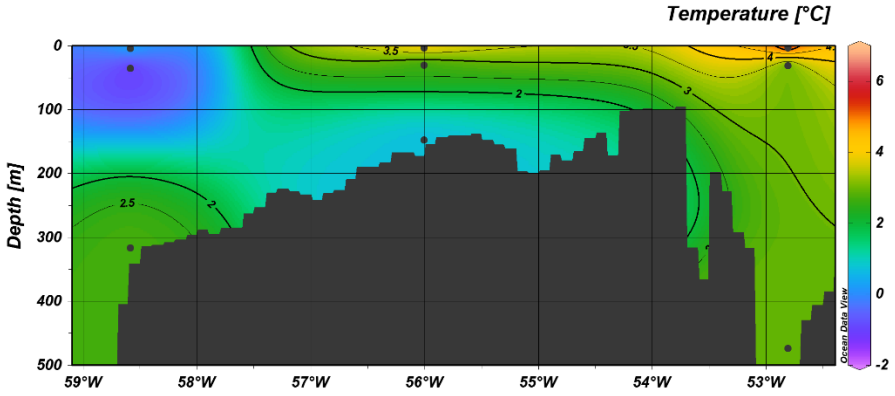

e) transect 5

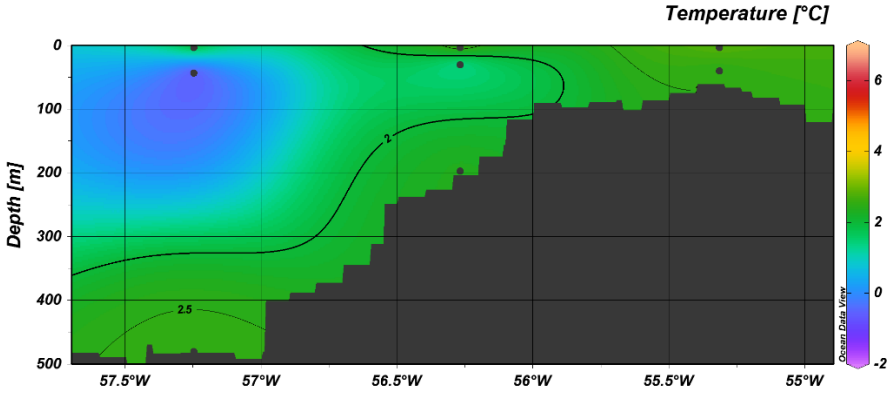

Figure 6 a - e. Temperature profiles of transects 1 – 5.

Salinity

Salinity increased with depth from 29.5 in the surface layers to 34.9 in deeper waters (Fig. 7). Along the longitudinal gradient, salinity generally remained stable, even though it would be expected that it is lower in near-shore stations due to meltwater input.

a) transect 1

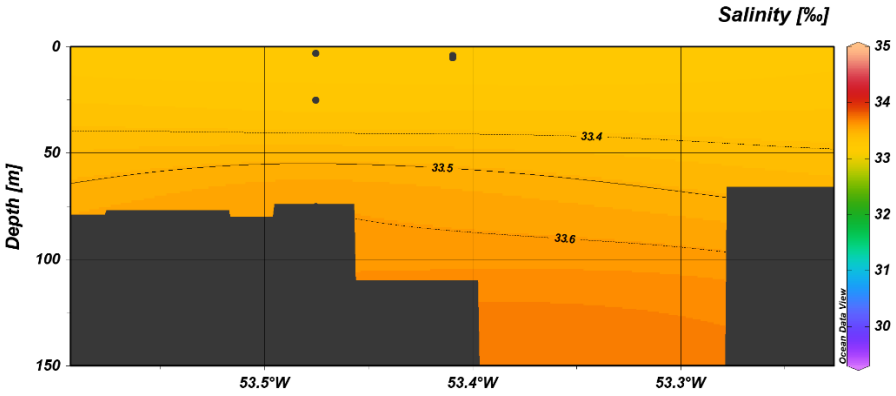

b) transect 2

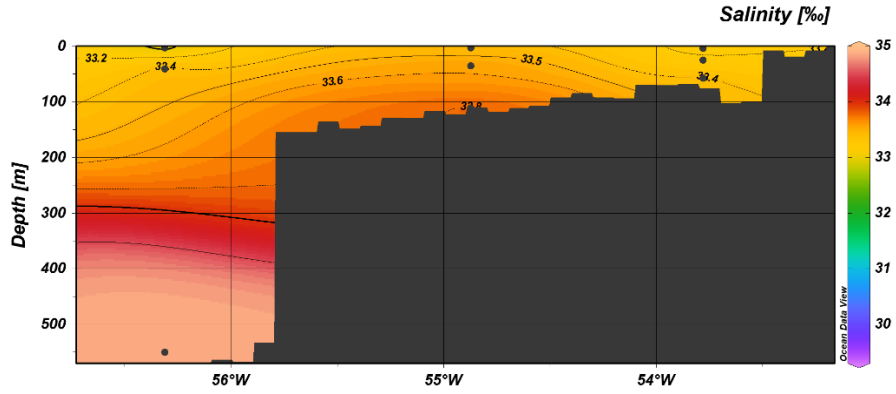

c) transect 3

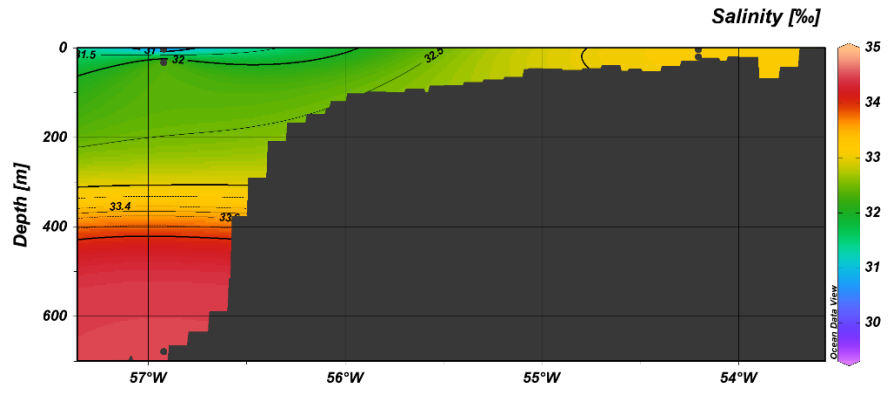

d) transect 4

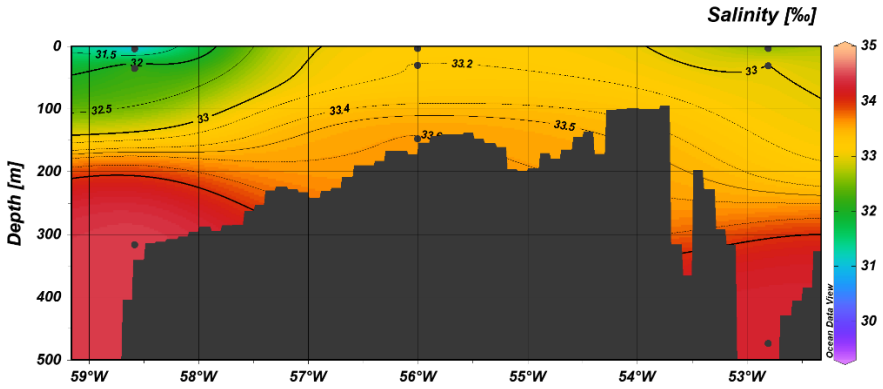

e) transect 5

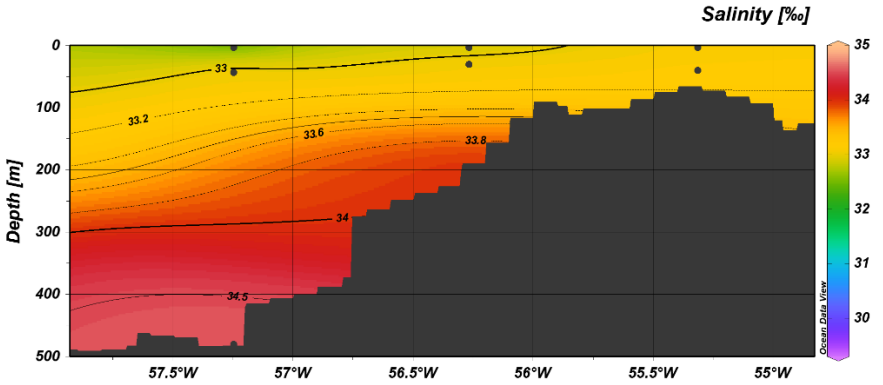

Figure 7 a – e. Salinity profile of transects 1 – 5.

Chlorophyll *a*

Chlorophyll *a* concentrations decreased with increasing depth and ranged between 0.014 to 0.087 µg/L. Highest concentrations were recorded within the top 100 m in the deep chlorophyll maximum which was present in transects 2 and 5 (Fig. 8 b, e). Chlorophyll *a* concentrations were stable (transects 1, 3 and 4) or higher at offshore then nearshore stations (transects 2 and 5).

a) transect 1

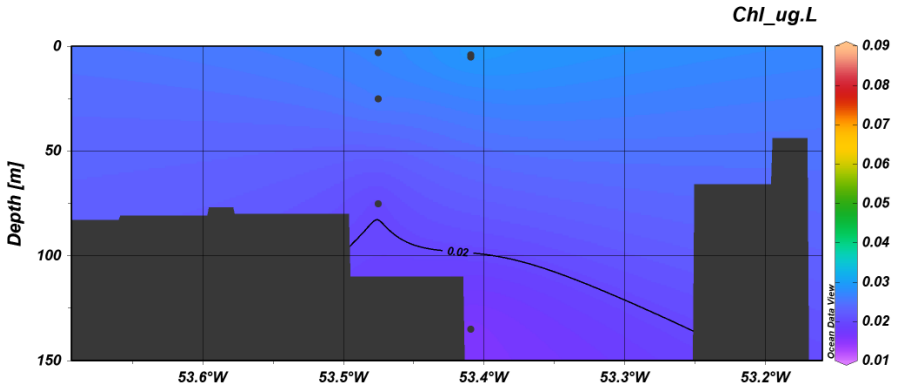

b) transect 2

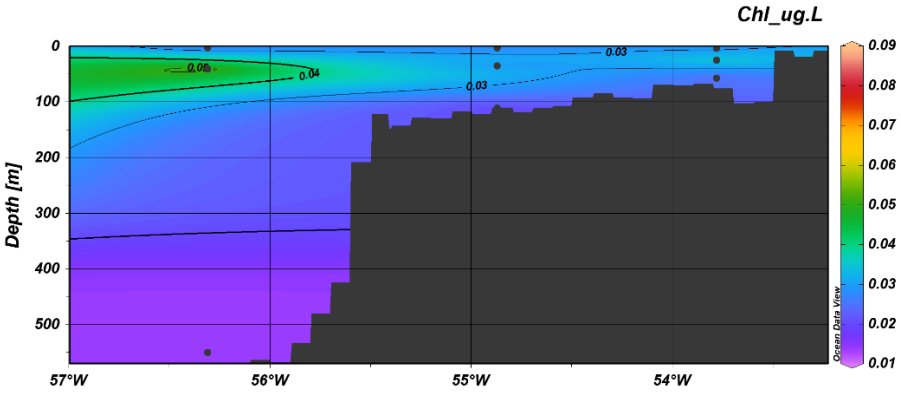

c) transect 3

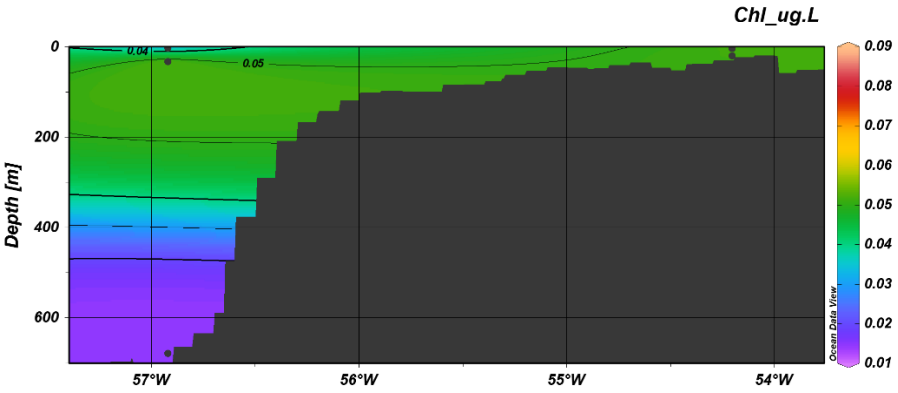

d) transect 4

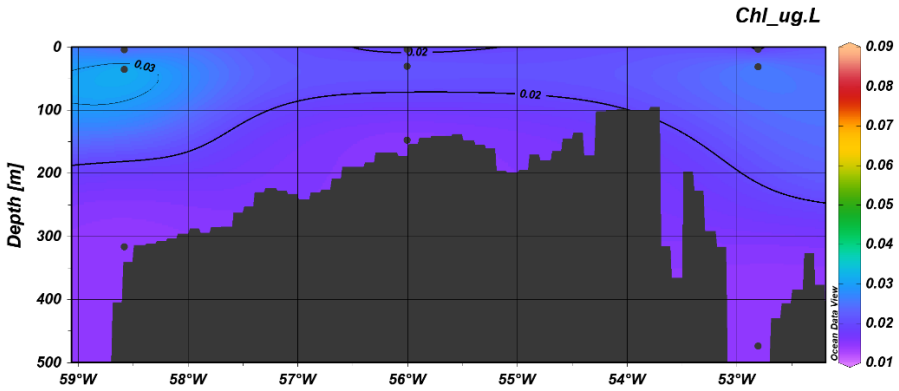

e) transect 5

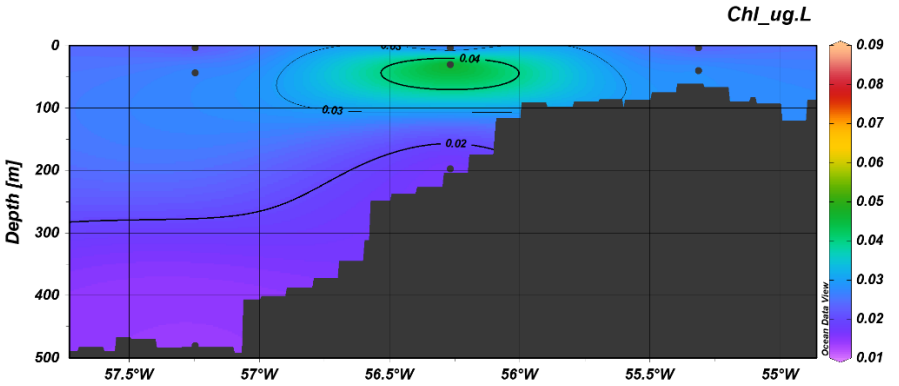

Figure 8 a – e. Chlorophyll a profiles of transects 1 – 5.

Oxygen

Oxygen concentrations decreased with increasing depth. Lowest recorded concentration was 203.41 µmol/L and the highest 388.74 µmol/L (Fig. 9). With the exception in transect 1, oxygen followed the chlorophyll concentrations.

a) transect 1

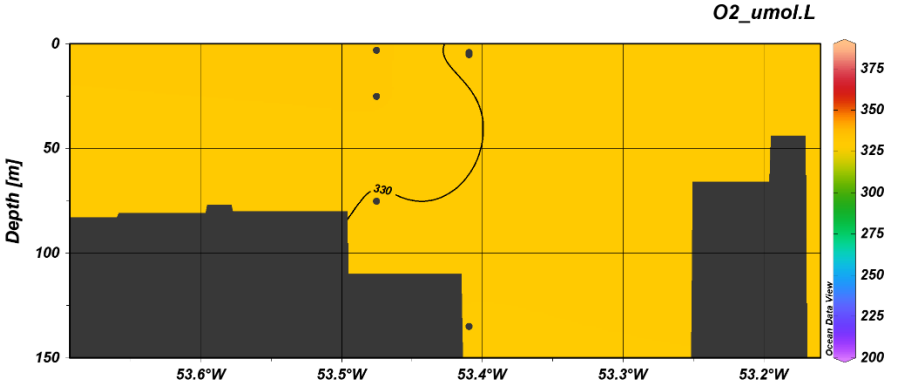

b) transect 2

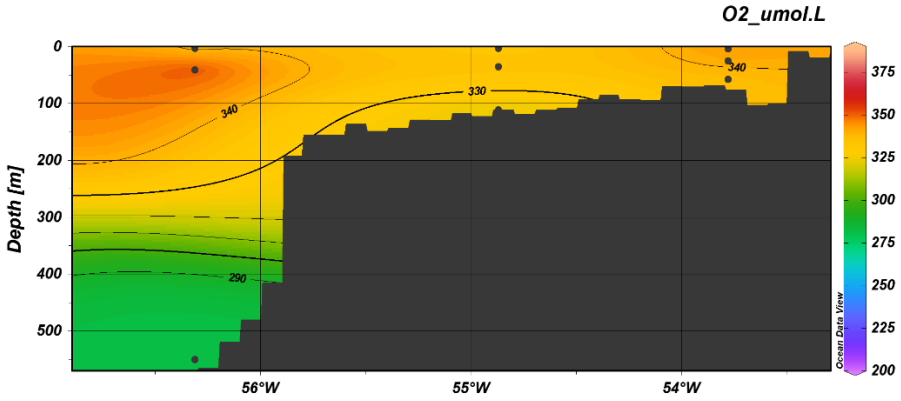

c) transect 3

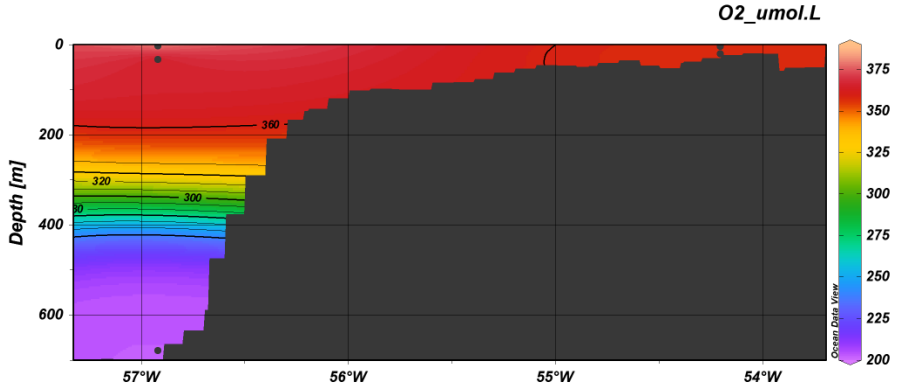

d) transect 4

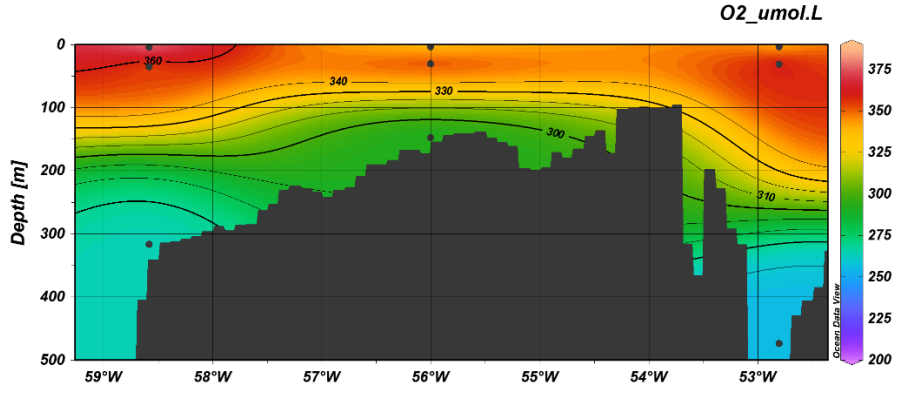

e) transect 5

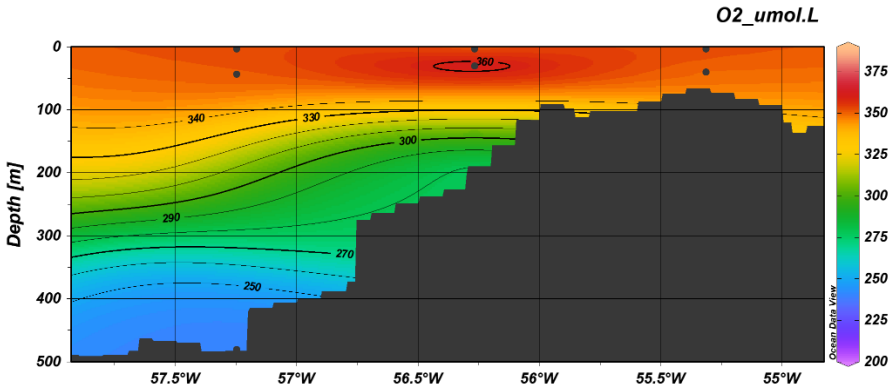

Figure 9 a – e. Oxygen profiles of transects 1 – 5.

Microbial abundance

Absolute abundance of prokaryotes

The prokaryotic abundance (PA) was determined at the stations 8, 10, 17, 21, 24, 26, 28, and 30 of the transects 2, 4 and 5. Generally, higher concentrations of prokaryotes were observed in the photic zone, ranging from 3 x 10^5 to 1.6 x 10^6 cells/mL, while a lower PA (less than 5 x 10^5 cells/mL) was noted below 200 meters (Fig. 10).

In transect 2, at the station 8, the highest PA was found in the surface waters (1.1 x 10^6 cells/mL) decreasing with depth. Lowest PA was noted at the DCM. At the station 10, the highest PA was found at the DCM (1.6 x 10^6 cells/mL), while in the surface and near-bottom waters the PA was lower.

In transect 4, at stations 17 and 24, representing the most inshore and offshore stations, respectively, PA was highest in the surface waters (>1.3 x 10^6 cells/mL) and gradually decreased with depth. Highest PA in the station 21 was found at the DCM (1.5 x 10^6 cells/mL), (Fig. 10).

At the station closest to the shore of the transect 5, station 26, PA remained relatively constant from the surface to the bottom (~1.0 x 10^6 cells/mL), which is likely due to the proximity of the sampling points in this shallow station. At station 28, highest PA was found at the DCM (7.3 x 10^5 cells/mL). At the station 30, highest PA was found in the surface waters (12.4 x 10^5 cells/mL) gradually decreasing with depth.

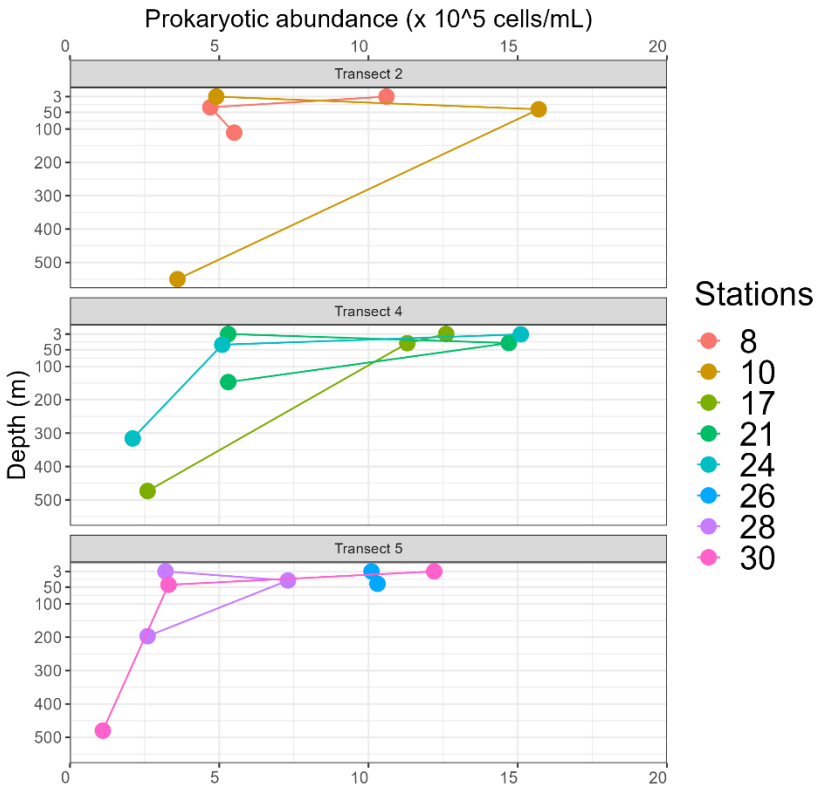

Figure 10. Prokaryotic abundance (cells/mL) at transects 2, 4 and 5.

Two different patterns in the vertical distribution of PA were observed. One found at stations 8, 17, 24 and 30 with the highest PA found in the surface waters, decreasing gradually with depth (with the exception at the DCM and near-bottom at station 8). The other pattern found at stations 10, 21 and 28 with highest PA at the DCM and lower PA at the other depths.

Abundance of *Alteromonas*

Alteromonas was found in every sample. Similarly to the PA, highest *Alteromonas* abundance (AA) and largest variability was found in the photic zone. Below 200 m less than 6.5 x 10^3 cells/mL were found (Fig. 11).

At station 8, highest AA was found in the surface waters decreasing towards the deeper waters where lowest AA was found in the DCM. At the offshore station of the transect 2, station 10, *Alteromonas* was most abundant in the DCM. The AA varied in the surface layers (1.3 x 10^4 - 6.6 x 10^4 cells/mL), while the abundance in the near-bottom waters remained rather constant (5.5 x 10^3 - 9.4 x 10^3 cells/mL).

Highest AA was detected at the DCM at station 10 and 21.

At the transect 5, at station 26, closest to the coast, highest AA was found in the surface waters (53.2 x 10^3 cells/mL). In contrast, AA was low at all depths of the station 28 (0.5 x 10^3 to 6.5 x 10^3 cells/mL). At the most offshore station of the transect, station 30, AA was decreased depth.

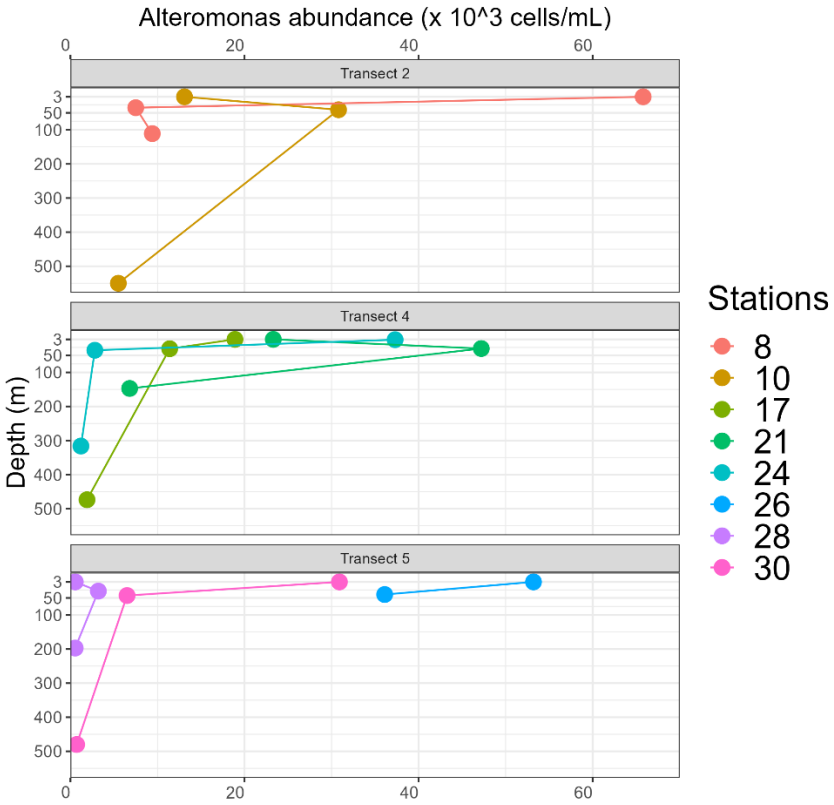

Figure 11. Alteromonas abundance (cells/mL) at the transect 2, 4 and 5.

The *Alteromonas* abundance relative to prokaryotic abundance along the three transects is shown in Figure 12. Highest relative AA was always found in the surface waters, with the only exception at station 28 where generally a low relative AA was recorded throughout the water column (<0.5 %).

a)

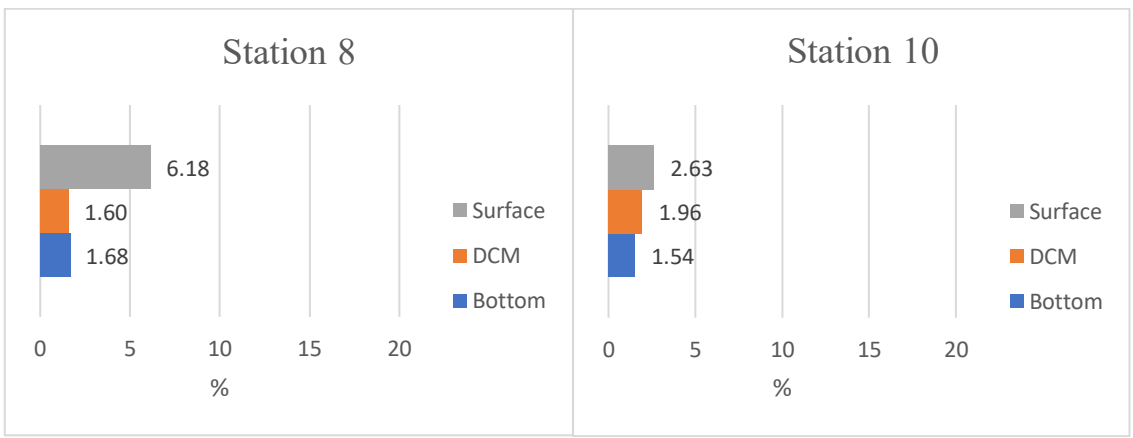

b)

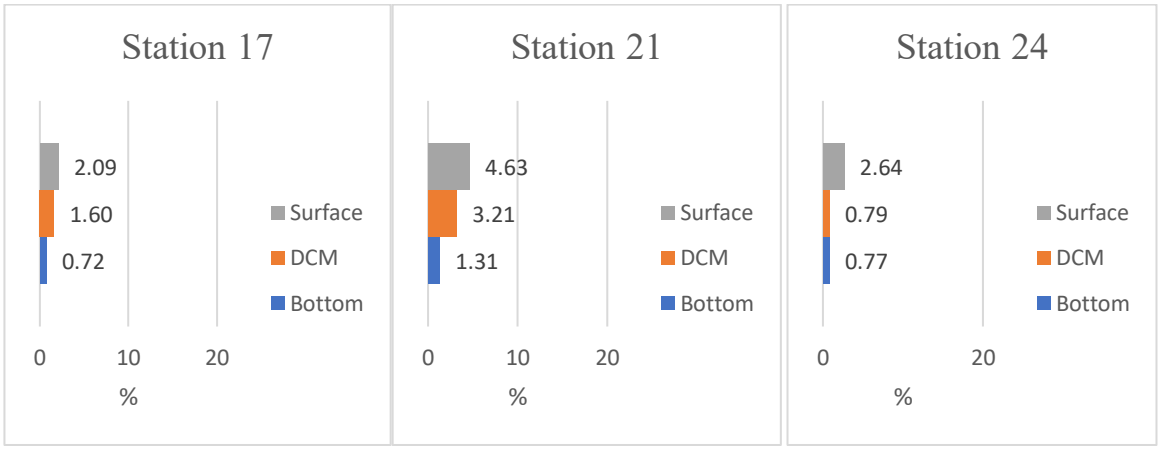

c)

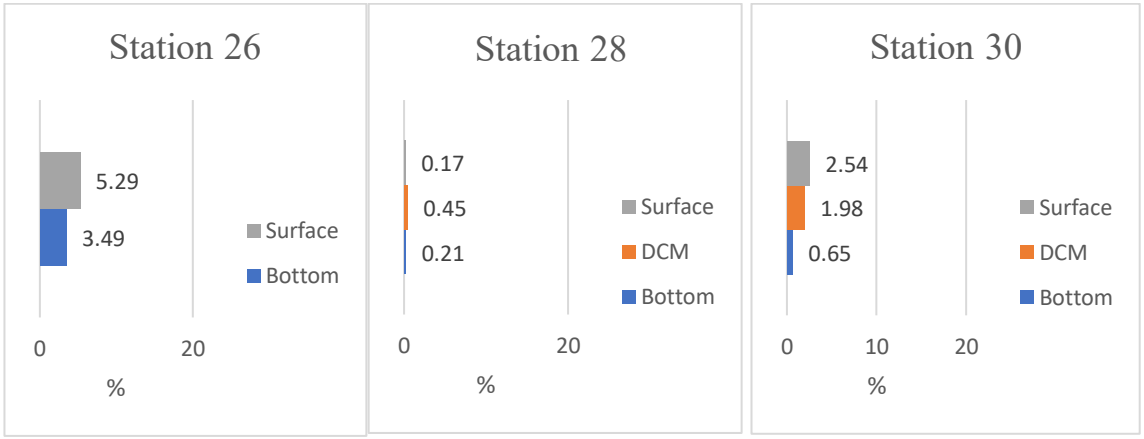

Figure 12. Alteromonas abundance as percentage of prokaryotic abundance. a) transect 2; b) transect 4; c) transect 5.

Microbial activity

Bulk microbial activity

Prokaryotic heterotrophic production (PHP) was measured by incorporation of ^{3}H-leucine at the stations 6, 8, 10, 11, 15, 17, 21, 24, 26, 28 and 30 of the transects 2 – 5. Generally, PHP varied significantly, ranging from 0.45 – 151.38 µmol C/m^3/d (Fig. 13).

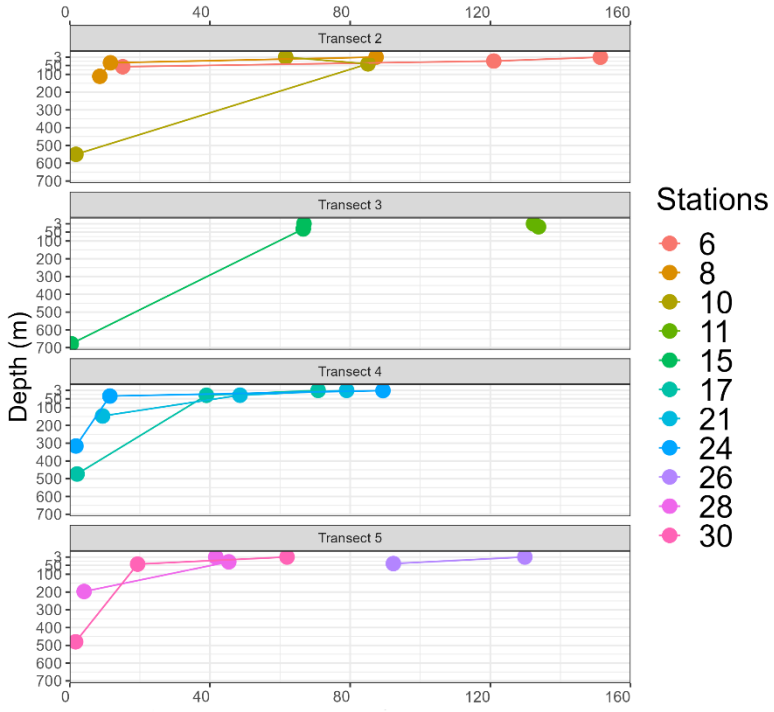

Figure 13. Bulk leucine incorporation at the 3 transects.

Bulk chemolithoautotrophic activity was measured by microbial fixation of ^{14}C-bicarbonate at the stations 10, 11, 15, 17, 21, 24, 26, 28 and 30 of the same transects. With exception at the station 10, autotrophic activity was more stable throughout all transects then heterotrophic activity. Highest activities were measured at the surface or DCM while lowest were measured always at near-bottom depth. Chemolithoautotrophic activity ranged between 0.5 and 76.4 µmol C/m^3/d (Fig. 14).

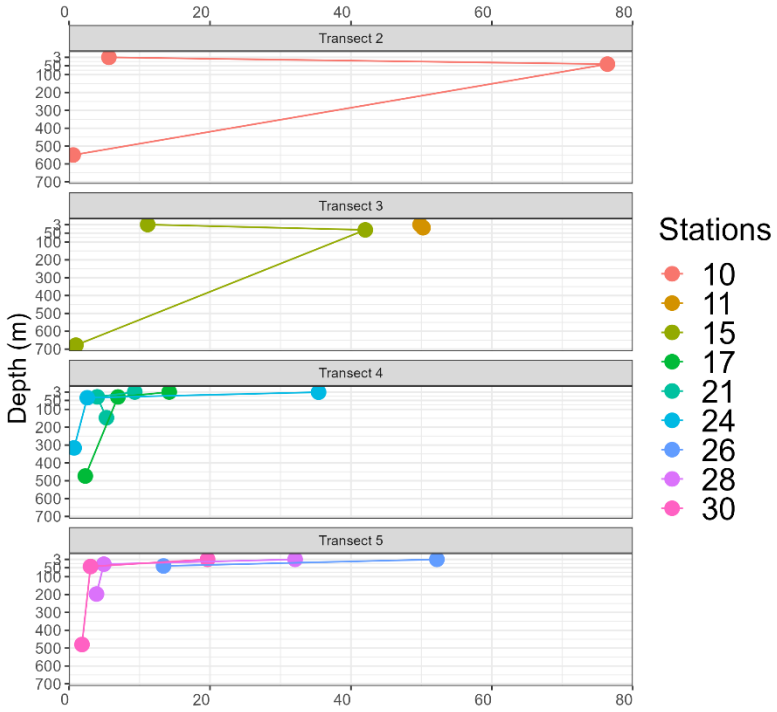

Figure 14. Bulk DIC fixation at the 3 transects.

The ratio between heterotrophic and chemolithoautotrophic bulk activity (PHP:DIC) is shown in Fig. 15. The ratio ranged between 0.4 – 12.2 and generally decresed with depth. With the exception in transect 3, the highest ratio was observed at the DCM.

a)

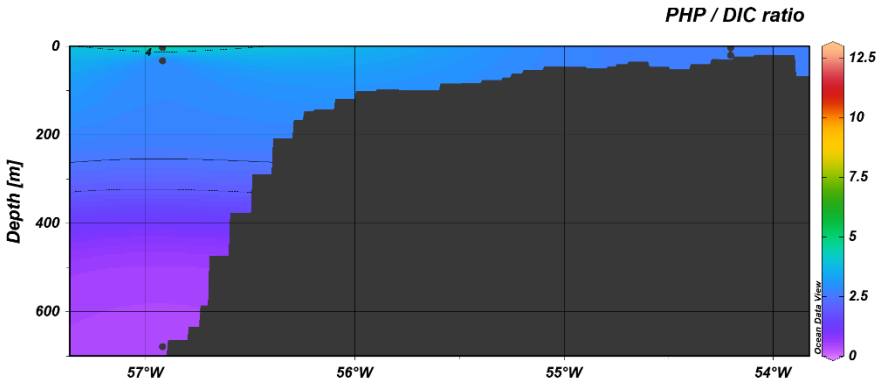

b)

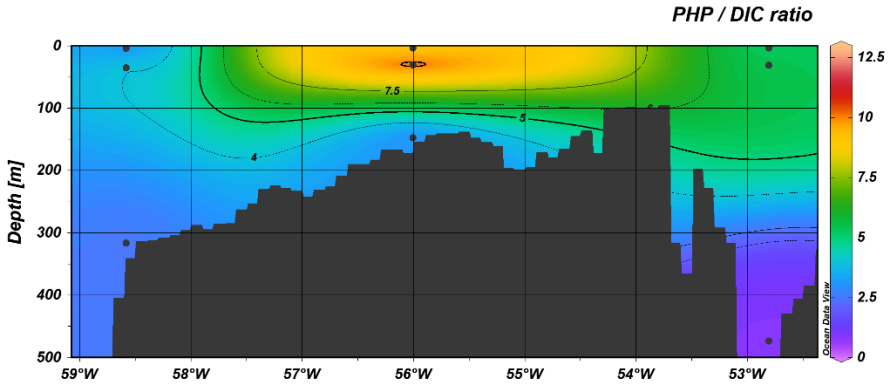

c)

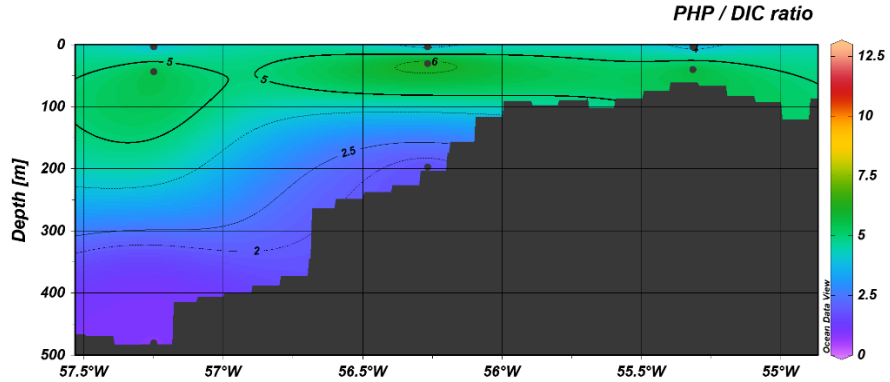

Figure 15. PHP to DIC ratio throughout the water column. a) transect 3; b) transect 4; c) transect 5.

Single-cell prokaryotic abundance

Abundance of leucine-positive cells

The abundance of leucine-positive cells, i.e., the number of cells taking up leucine as determined by microautoradiography linked to fluorescent in situ hybridization was estimated at stations 8, 10, 17, 21, 24, 26, 28 and 30 of the transects 2, 4 and 5. Results are shown as percentage of: active prokaryotes (leucine-positive) cells to total prokaryotic abundance (Fig. 16), leucine-positive *Alteromonas* to leucine-positive prokaryotes (Fig. 17) and leucine-positive *Alteromonas* as percentage of total *Alteromonas* abundance (Fig. 18).

In general the percentage of leucine-positive prokaryotes ranged from 14 to 85 %. Lowest activity was found in transect 2, station 10 and near-bottom depth of station 8. Interestingly, deep-est layer sampled at station 10 had the highest percentage of leucine-positive cells within that station. All the other samples revealed >50 % of leucine-positive prokaryotes. Most of the samples had between 50 and 75 % of active prokaryotes (Fig 16).

The contribution of *Alteromonas* leucine-positive cells to leucine-positive prokaryotes was generally low ranging from 0.2 to 6.1 %. The lowest percentage of leucine-positive *Alteromonas* was found mainly at near-bottom depth, while the highest percentage was typically found at the DCM layer (stations 21, 26 and 30), (Fig. 17).

The percentage of leucine-positive *Alteromonas* cells of total *Alteromonas* cells was generally high, indicating that the major fraction of the *Alteromonas* population was heterotrophically

active. Leucine-positive cells *Alteromonas* amounted to 30 to 100 % of the total *Alteromonas* population (Fig. 18).

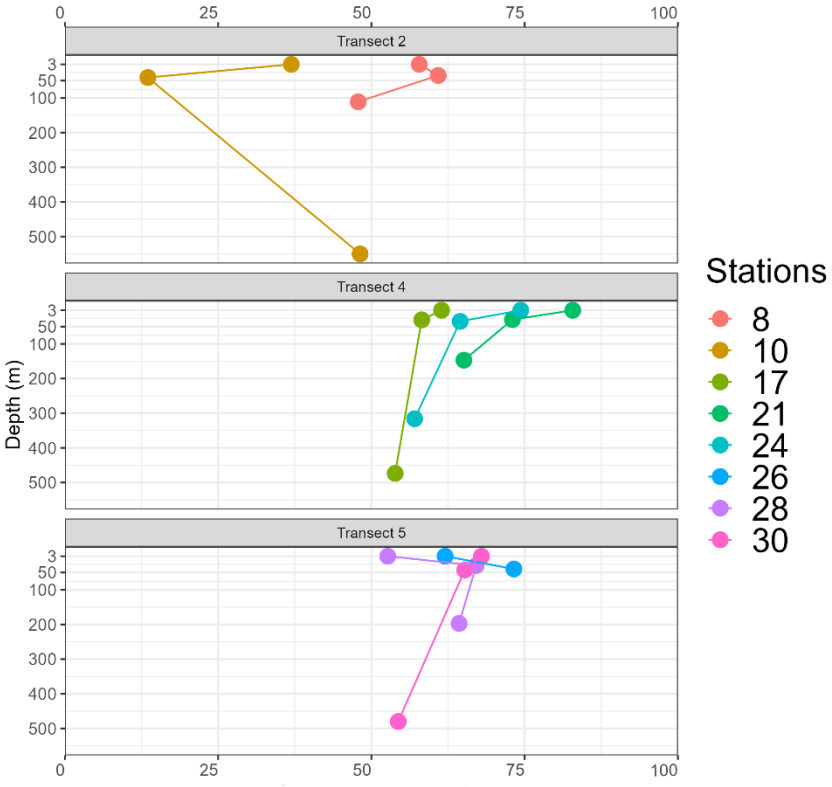

Figure 16. Leucine-positive prokaryotic as percentage of total prokaryotic abundance.

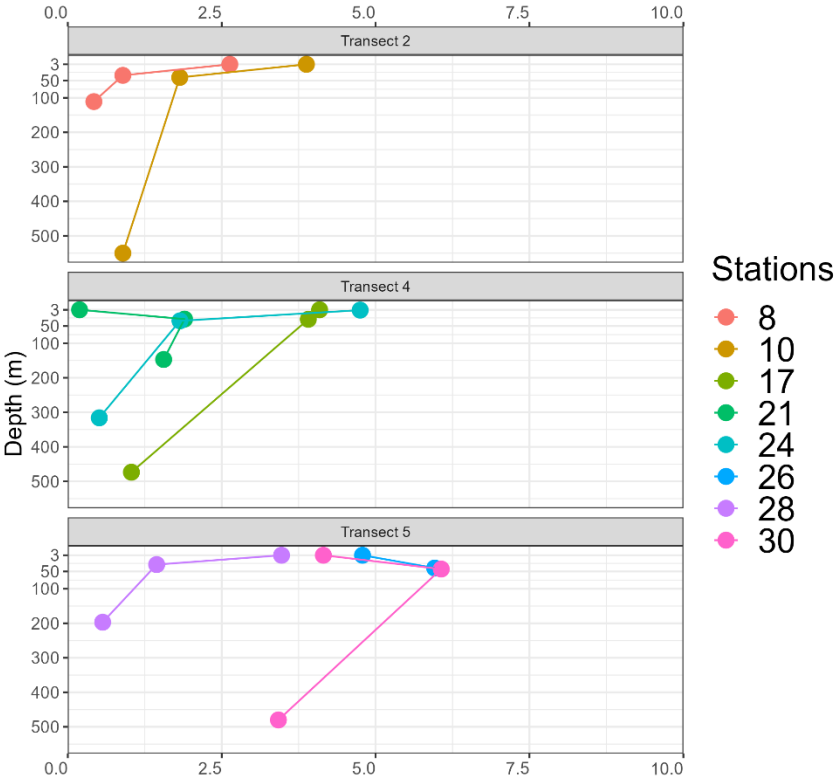

Figure 17. Leucine-positive Alteromonas cells as percentage of total leucine-positive prokaryotes.

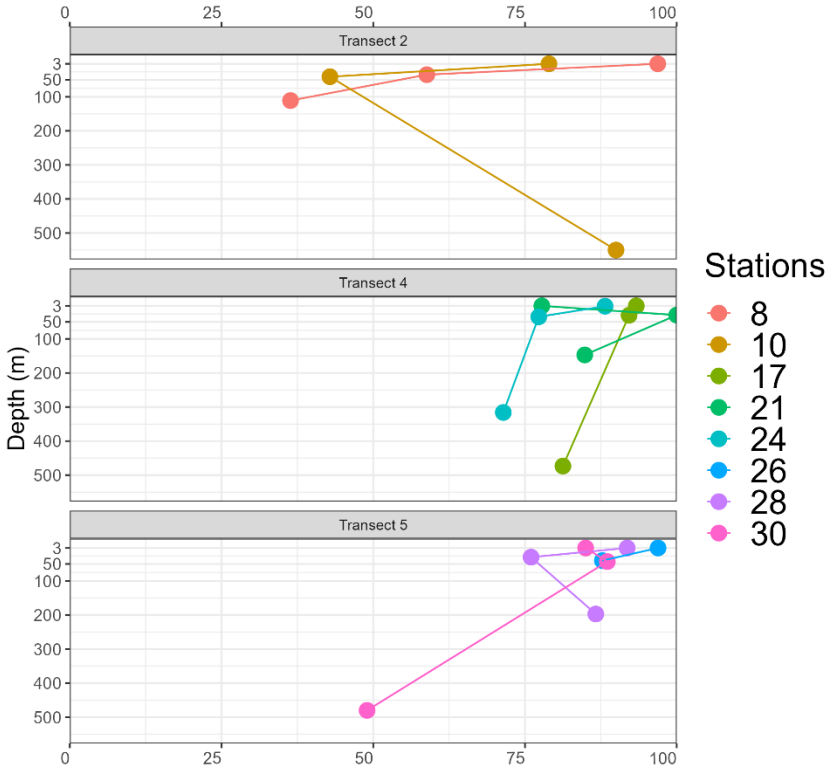

Figure 18. Leucine-positive Alteromonas cells as percentage of total Alteromonas cells.

Abundance of DIC-positive cells

The abundance of DIC-postive cells using ^{14}C-bicarbonate was determined at stations 10, 17, 24, 26, 28 and 30 of the transects 2, 4 and 5. Results are presented as the percentage of: DIC-positive prokaryotes to prokaryotic abundance (Fig. 19), DIC-positive *Alteromonas* cells to DIC-positive prokaryotes (Fig. 20) and DIC-positive *Alteromonas* cells to total *Alteromonas* abundance (Fig. 21).

The abundance of DIC-positive cells was generally lower than the abundance of leucine positive cells. In all samples, at least ~ 10 % of the cells were DIC-positive reaching up to 45 % of the total prokaryotic cells (station 28). At stations 10 and 17, similar pattern is observed (Fig. 19).

DIC-positive *Alteromonas* cells contributed between 0 to 8.5% to the total DIC-positive prokaryotes. In four samples (stations 17 and 24), all belonging to transect 4, no DIC positive *Alteromonas* cells were detected, while the highest percentages of DIC-positive *Alteromonas* were found at station 26. There was no clear pattern between depth and DIC-positive cells among any stations (Fig. 20).

The variability observed in the percentage of DIC-positive *Alteromonas* to total *Alteromonas* population was much larger than in leucine-positive *Alteromonas* (Fig. 21).

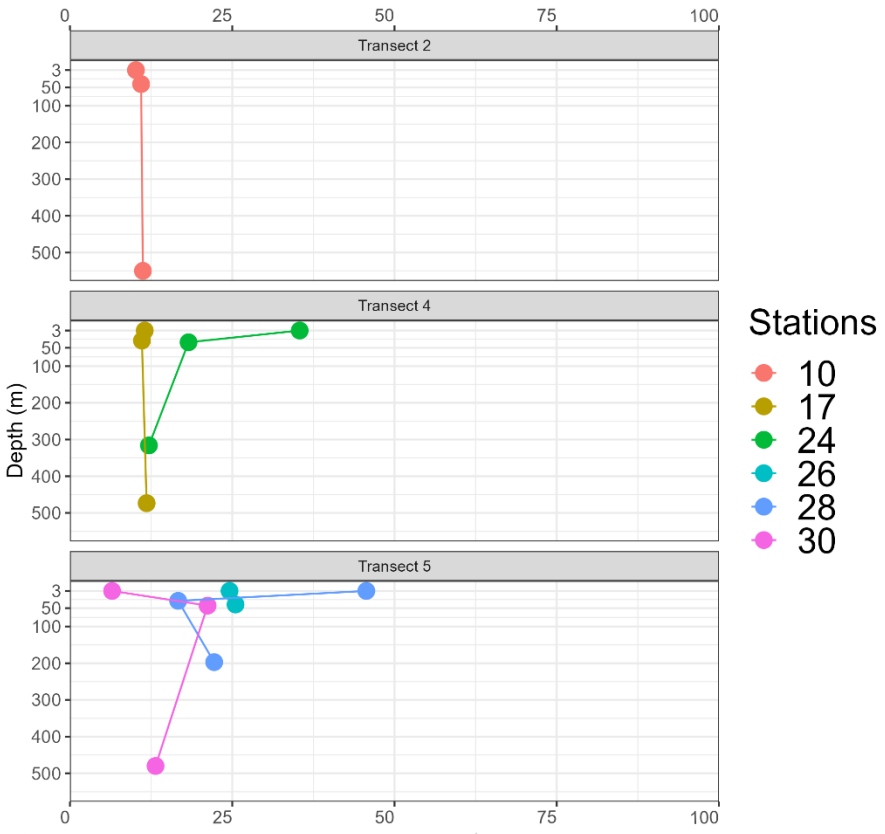

Figure 19. DIC-positive prokaryotes as percentage of total prokaryotic abundance.

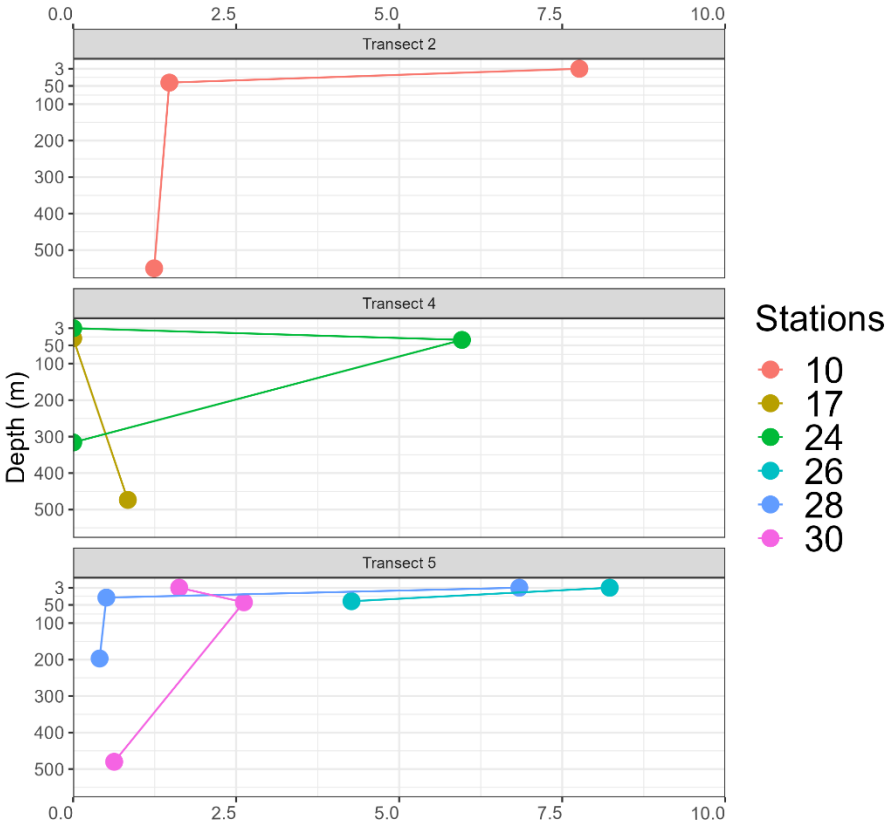

Figure 20. DIC-positive Alteromonas as percentage of DIC-positive prokaryotes.

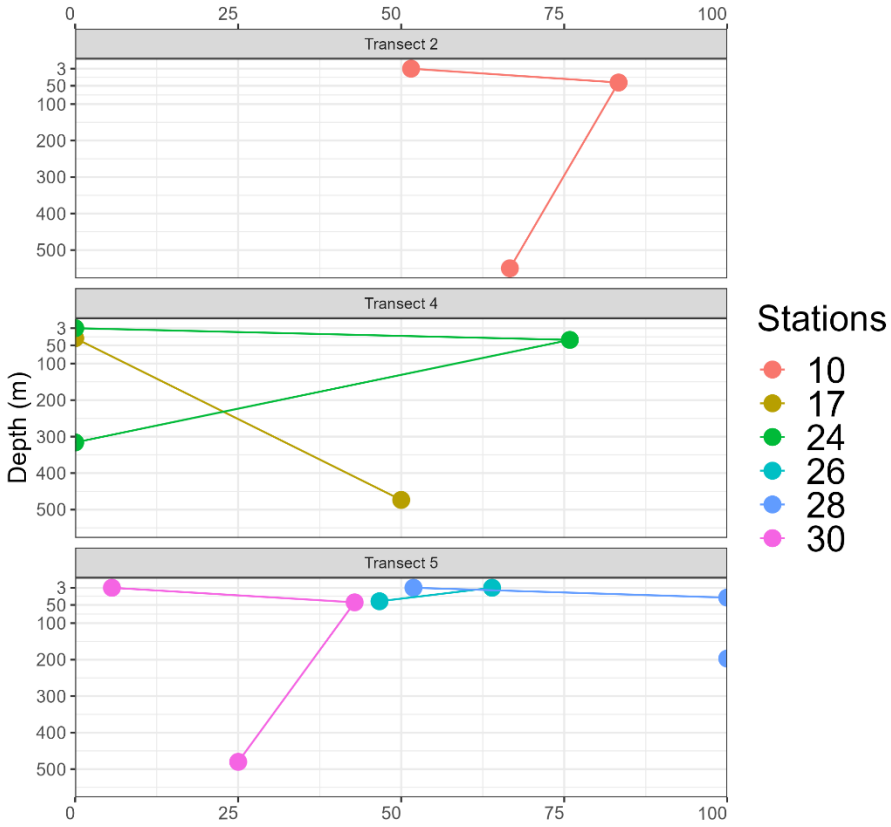

Figure 21. DIC-positive Alteromonas as percentage of total Alteromonas abundance.

Single-cell activity

Single cell activity was calculated by relating total silver grain area to the bulk activity measured by ^{3}H leucine or ^{14}C bicarbonate incorporation of the bulk community.

^{3}H-leucine uptake by prokaryotes

Leucine uptake by single prokaryotic cells (DAPI +) ranged between 10.27 and 14.83 amol leucine/cell/h (Fig. 22). Almost 50 % of cells incorporated between 12.55 and 13.69 amol leucine/cell/h. Single-cell activity was rather uniform throughout the water column and transects.

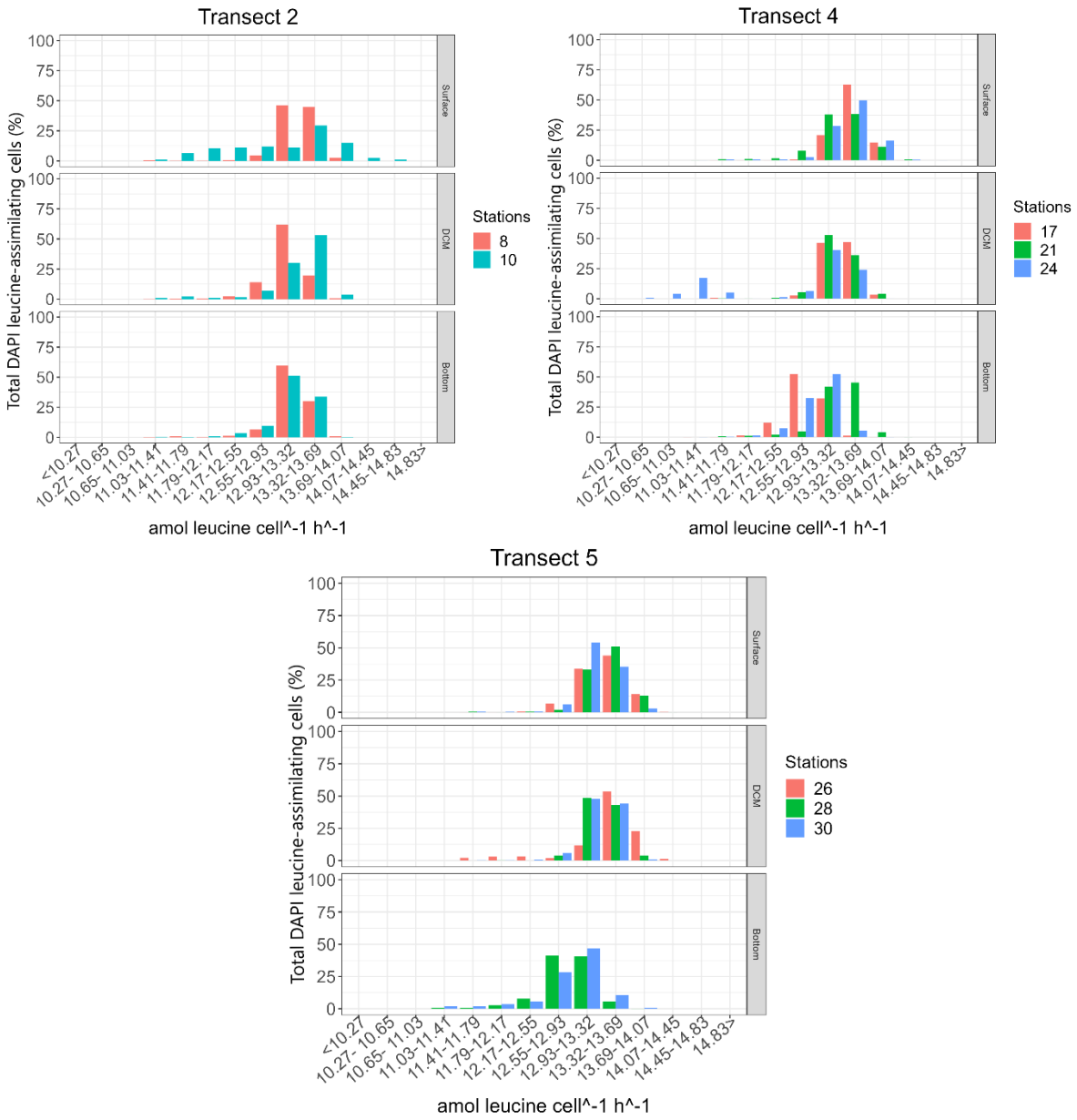

Figure 22. Leucine uptake of DAPI stained cells for transects 2, 4 and 5.

^{3}H-leucine uptake by *Alteromonas*

The contribution of *Alteromonas* cells to total prokaryotic activity was low. The single cell activity levels of *Alteromonas* varied more than the single-cell activity levels of the total prokaryotic community (Fig. 23). Similarly to the single cell prokaryotic activity, in half of the samples most cells incroporated between 13.32 and 14.07 amol leucine/cell/h meaning that *Alteromonas* was very active. Generally, the contribution of *Alteromonas* cells to total prokaryotic activity was higher in the surface waters than in the deeper layers of the water column.

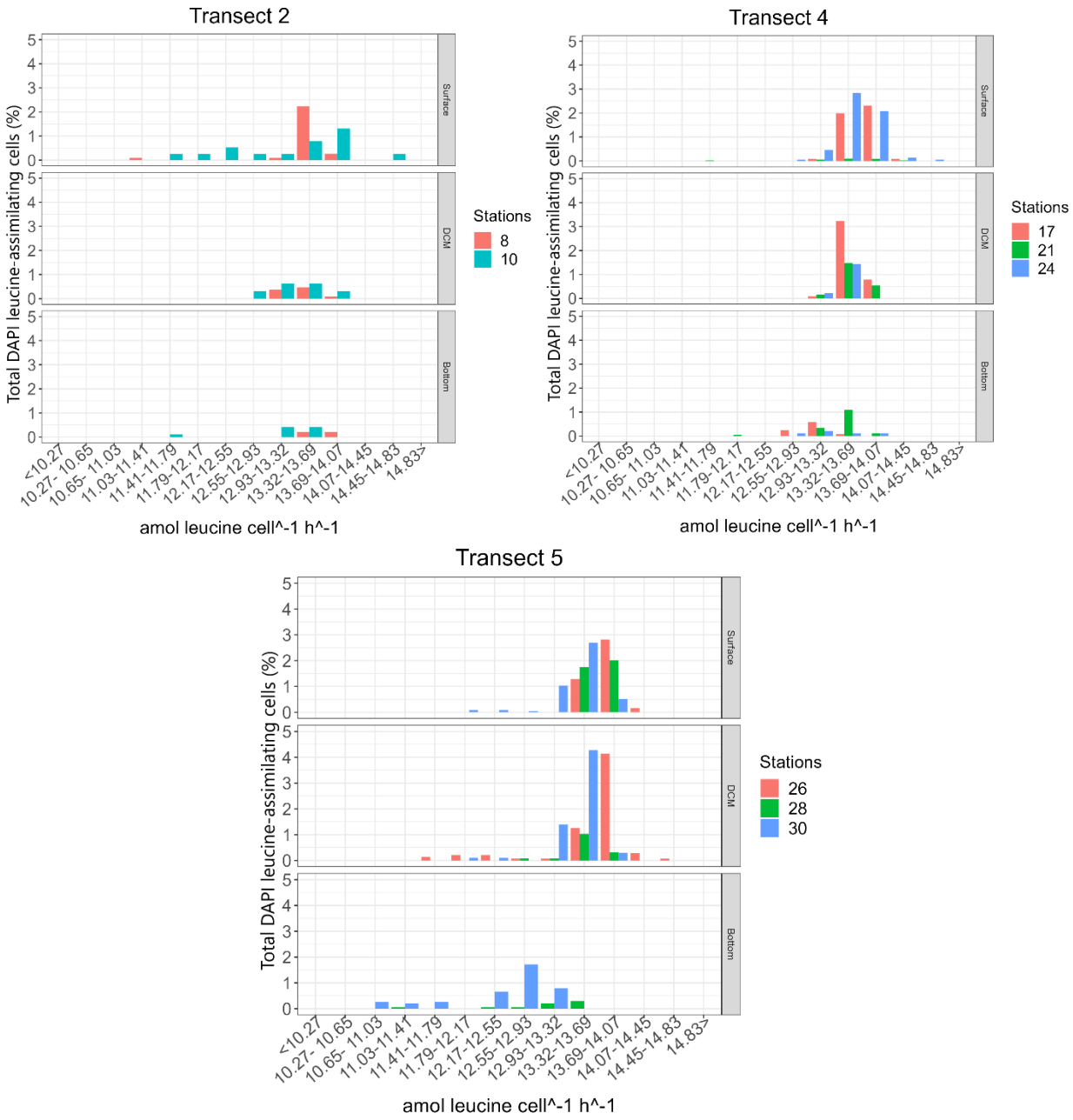

Figure 23. Leucine uptake of Alteromonas cells as percentage of the leucine uptake of total DAPI stained cells in the different depth layers.

^{14}C-bicarbonate fixation by prokaryotes on a single-cell level

Chemolithoautotrophic activity of prokaryotic cells ranged between 0.71 and 4.04 fmol DIC/cell/h (Fig. 24). A bell-shaped distribution of activity was observed but was less pronounced since activity varied much more than heterotrophic activity as determined by ^{3}H-leucine. At most of the stations, the highest percentage of cells DIC fixation per cell amounted between 1.32 and 1.92 fmol DIC/cell/h.

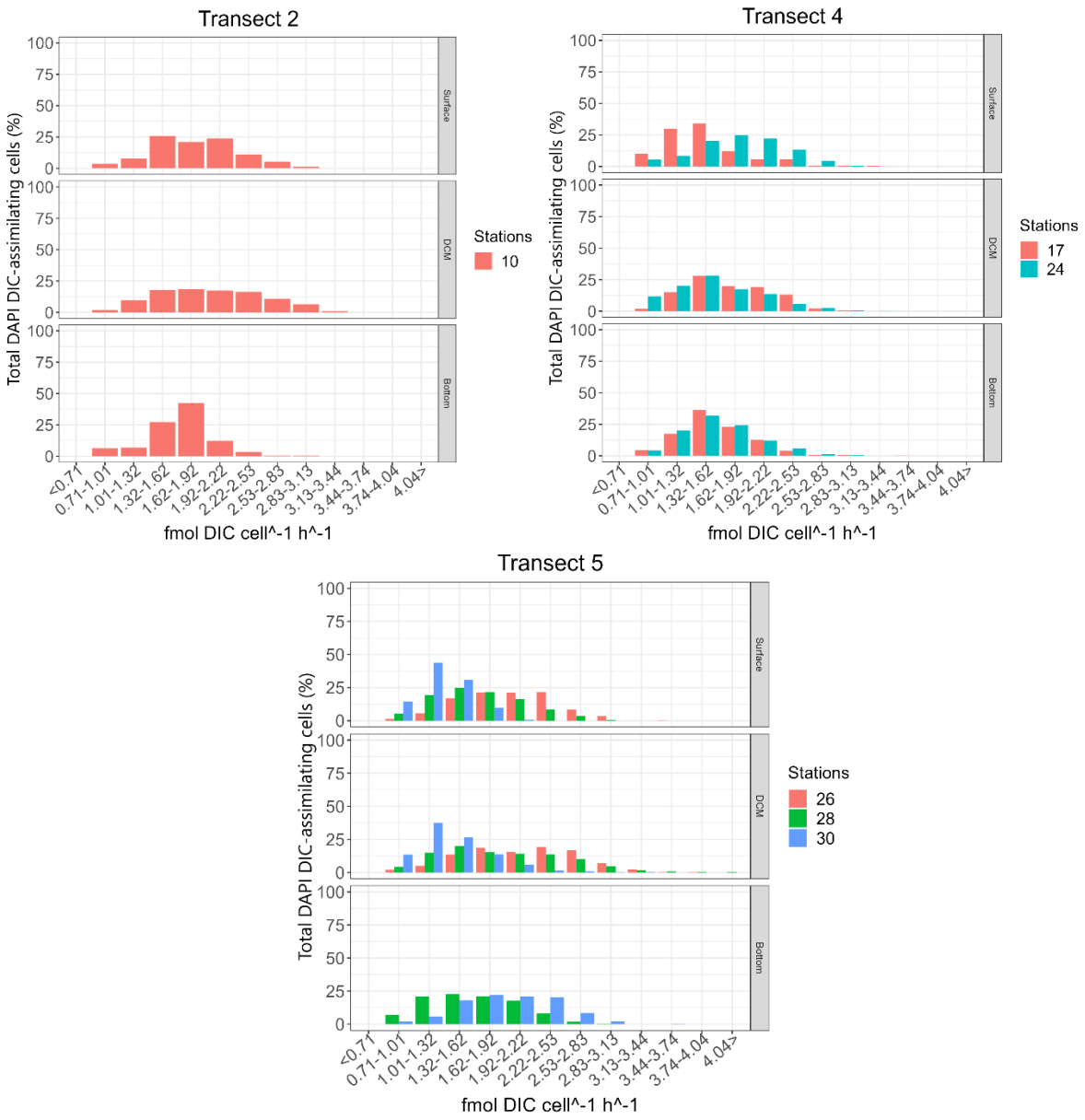

Figure 24. DIC fixation of DAPI + cells on a single cell level.

^{14}C-bicarbonate fixation by *Alteromonas* on a single-cell level

Alteromonas cells varied in their activity tremendously; out of six samples in transect 4, only in two were active *Alteromonas* cells detected. Highly active cells were present in the surface waters of station 10 (Fig. 25).

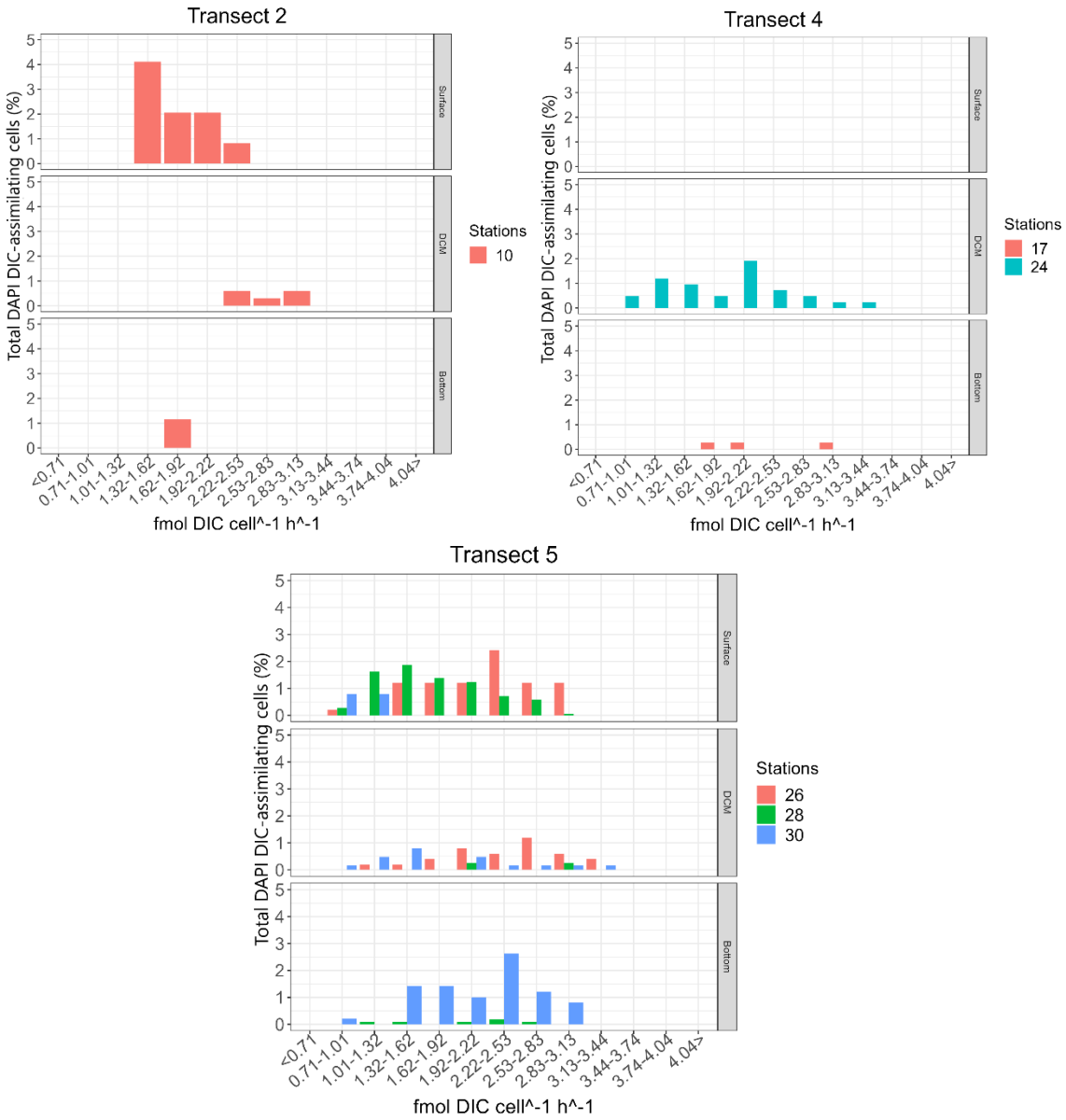

Figure 25. DIC fixing Alteromonas cells as a percentage of total prokaryotes fixing DIC.

The contribution of *Alteromonas* to total prokaryotic heterotrophic and chemolithoautotrophic activity is shown in Table 1. Leucine uptake of *Alteromonas* ranged between 1.13 to 11.35 % to total leucine uptake, while DIC fixation ranged between 0 – 18.83 % to total prokaryotic DIC fixation (Table 1).

Table 1. Contribution of Alteromonas to total prokaryotic heterotrophic and autotrophic activity in the surface, DCM layer and bottom waters.

Layer	Station	^{3}H-leucine	^{14}C-bicarbonate
Surface	8	4.26	NA
	10	7.41	10.77
	17	7.39	NA
	21	0.42	NA
	24	9.16	NA
	26	9.01	13.50
	28	6.68	9.47
	30	6.56	0.70
		6.36 ± 2.85	8.61 ± 5.53
DCM	8	1.59	NA
	10	2.22	3.88
	17	7.03	NA
	21	4.19	NA
	24	3.75	18.83
	26	11.35	6.76
	28	2.50	1.04
	30	7.75	13.05
		5.05 ± 3.38	8.71 ± 7.20
Near bottom	8	1.13	NA
	10	1.13	0.97
	17	1.43	3.53
	21	2.18	NA
	24	1.17	NA
	28	1.37	1.50
	30	4.52	13.50
		1.85 ± 1.23	4.87 ± 5.86

Discussion

Dynamics in microbial abundance

The decrease in microbial abundance with increasing depth is commonly found in marine ecosystems due to the decreasing organic matter availability with depth (Schauberger et al, 2021). In a study carried out in the summer season in the Chukchi Sea, which is one of the areas in the Arctic Ocean with the highest productivity (Kwon et al, 2022), the prokaryotic abundance varied between 0.8 and 8.7 x 10^5 cells/mL in the surface waters (Hodges et al, 2005) and are therefore somewhat lower than in our study (Fig. 10) The higher abundance found in the surface waters off West Greenland might indicate elevated input from the terrestrial environment.

We expected that inshore stations have higher abundance of *Alteromonas* due to generally higher nutrient and DOM concentrations near the coast which favour copiotrophics such as *Alteromonas.* Overall, a high abundance of *Alteromonas* was found at inshore stations (Fig. 11). Interestingly, stations 10 and 21, where the highest abundance of *Alteromonas* was found at the DCM were located at similar longitudes (Fig. 3). This similar vertical distribution of *Alteromonas* at the different latitudinal stations may indicate the influence of northward (WGC) or southward water flow (BIC; coined Polar Water (Buch, 2002).

In marine surface waters, the DOM composition determines the activity of prokaryotes (Pontiller et al., 2020). Summer in the Arctic (April - September) is usually a period with high primary productivity in the Arctic (Wassmann, 2011). Sunlight and mixing of the nutrients provide favourable conditions for primary producers. These primary producers provide labile DOM to heterotrophic prokaryotes including *Alteromonas*. Our samples collected in July potentially reflect these conditions leading to the high abundance of *Alteromonas* in this region. David Strait is the area where Baffin Island Current and West Greenland Current meet. DOM transported from the south via the WGC to the coastal waters of Greenland could affect the distribution of *Alteromonas.* Another source of DOM is terrestrial input. We found high *Alteromonas* abundance at some inshore stations (Fig. 11) along the transects potentially influenced by river runoff.

In the context of changing climate, temperature and salinity are important parameters in Arctic systems (Kirchman et al., 2009). Generally, microbial growth increases with rising temperature (Starosick and Smith, 2004). Melting of the ice glaciers releases freshwater into the oceans, decreasing its salinity. At the study sites, salinity was generally increasing with depth. *Alteromonas* was more abundant under lower salinity. We hypothesize that a further temperature increase will lead to the expansion of primary production and therefore of heterotrophic bacterial production, including growth of *Alteromonas.*

Microbial activity

Generally, bulk prokaryotic heterotrophic production and chemolithoautotrophic activity decreased with increasing depth (Figs. 13, 14), which is explained by reduced bioavailability of DOM with depth and reduced availability of inorganic reduced compounds potentially serving as electron donors, respectively. Prokaryotic heterotrophic production (PHP) and DIC fixation correlated (Fig. 26). A positive correlation might indicate DIC fixation by heterotrophs via anaplerotic reactions (Guerrero-Feijóo et al., 2018).

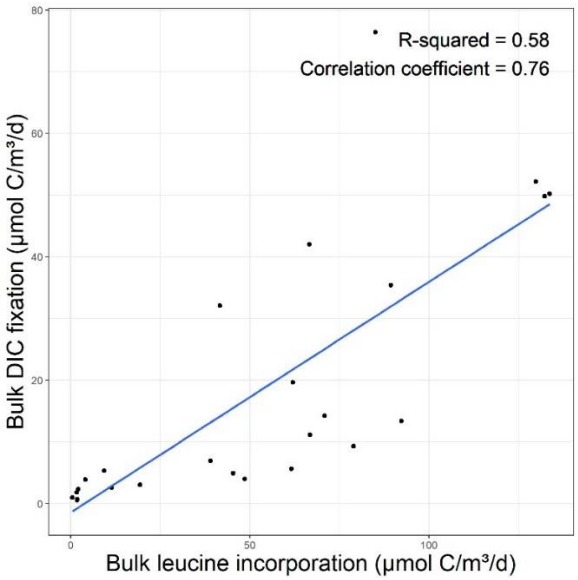

Figure 26. Relationship between bulk leucine incorporation and DIC fixation.

Comparing these results to a similar study in the waters of the North Atlantic Deep Water, Reinthaler et al. (2010) reported a decrease from surface to the mesopelagic waters of both PHP (from 7.45 to 0.07 µmol/m^3/d) and DIC fixation rate (from 3.33 to 0.08 µmol/m^3/d). Furthermore, they found higher DIC fixation rates than PHP throughout the water column in the eastern basin of the North Atlantic, while DIC fixation rates were lower in the western basin of the North Atlantic (except in the subsurface waters). In our study, we found higher DIC fixation rates than PHP only in some near bottom waters (Fig. 15). DIC fixation rates were more stable throughout the water column than PHP (Fig. 15).

The highest percentage of leucine positive *Alteromonas* contributing to PHP was obtained for the photic zone (Fig. 17). The contribution of leucine positive *Alteromonas* to total *Alteromonas* abundance was > 75 % at more than a half of the stations and leucine incorporation on a single-cell level of *Alteromonas* was high (13.32 and 14.07 amol leucine/cell/h) indicating very high heterotrophic activity (Fig. 18).

In contrast, the contribution of DIC positive *Alteromonas* to total prokaryotic DIC fixation was more variable, ranging from no autotrophic *Alteromonas* to 18.8 %, with no clear depth pattern (Fig 20). Comparing these results to the study in the Atlantic (Guerrero-Feijóo et al., 2018), *Alteromonas* contributed 2 % to the total DIC fixation there, which is lower than what we found (7.4 % on average throughout the water column) (Table 1). The high variability of chemolithoautotrophic activity of *Alteromonas,* not just between the station and transects, but also at the same depth layers, makes it difficult to estimate the importance of the chemoautotrophy or anaplerotic metabolism of *Alteromonas* in the Arctic Ocean. Tentatively, we conclude that *Alteromonas* is not mixotroph but that the DIC fixation we measured is caused by anaplerotic metabolism of highly heterotrophically active *Alteromonas* cells.

Conclusion

The abundance and activity of *Alteromonas* in the waters off West Greenland was studied to elucidate the contribution of the DIC fixation by heterotrophs and better understand microbial processes in the fragile ecosystem, the marine Arctic. Our results show that ratio of heterotrophic to chemolithoautotrophic activity is highest in the photic zone and lowest (< 1) in the bottom waters. *Alteromonas* contributed between 4.9 to 8.7 % to the total prokaryotic DIC fixation. We hypothesize that climate change will promote the expansion of *Alteromonas* and that *Alteromonas* could play a significant role in the DIC fixation in this region. Recent estimates suggest that heterotrophic DIC fixation contributes between 1 and 5 % to carbon biomass production (Braun et al., 2021) and our findings indicate that *Alteromonas* should be included in future inorganic carbon cycling estimations.

Bibliography

Acinas, S.G., Antón, J., and Rodríguez-Valera, F. Diversity of free-living and attached bacteria in offshore Western Mediterranean waters as depicted by analysis of genes encoding 16S rDNA. *Applied Environmental Microbiology*, 65: 514–522 (1999).

Amano, C., Zihao, Z., Sintes, E., Reinthaler, T., Stefanschitz, J., Kisadur, M., Utsumi, M., Herndl, G J., Limited Carbon Cycling Due to High-Pressure Effects on the Deep-Sea Microbiome. *Nature Geoscience,* 15, pages 1041–1047 (2022).

Baltar, F., Aristegui, J., Gasol, J. M., Sintes, E., Herndl, G. J. Evidence of prokaryotic metabolism on suspended particulate organic matter in the dark waters of the subtropical North Atlantic. *Limnology and Oceanography,* 54 (1): 182 – 193 (2009).

Baumann, P. Bergey‘s Manual of Systematic Bacteriology. *Williams & Wilkins Co, Baltimore*, Vol. 3: 243–354 (1972).

Behera, P., Tiwari, M., Knies, J. Enhanced Arctic stratification in a warming scenario; evidence from the mid Pliocene warm period. *Advancing Earth and Space Sciences,* Vol. 36 (6) (2021).

Braun, A., Spona-Friedl, M., Avramov, M., Elsner, M., Baltar, F., Reinthaler, T., Herndl, G. J., Griebler, C. Reviews and syntheses: Heterotrophic Fixation of the Inorganic Carbon – Significant But Invisible Flux in Environmental Carbon Cycling. *Biogeosciences,* Vol. 18 (12): 3689 – 3700 (2021).

Buch, E. Present Oceanographic Conditions in Greenland Waters. Copenhagen: Danish Meteorological Institute, 1 – 36 (2002).

Guerrero-Feijóo E, Sintes E, Herndl GJ, Varela MM. High dark inorganic carbon fixation rates by specific microbial groups in the Atlantic off the Galician coast (NW Iberian margin). *Environmental Microbiology*, 20 (2): 602-611 (2018).

Heinze, C., Bleckner, T., Martins, H., Rusiecka, D., Döscher, R., Gehlen, M., Gruber, N., Holland, E., Hov, O., Joos, F., Matthews, J. B. R. The quiet crossing of ocean tipping points. *Proc. Natl. Acad. Sci.* Vol. 118 (9) (2021).

Herndl, G.J., Reinthaler, T., Teira, E., van Aken, H., Veth, C., Pernthaler, A., Pernthaler, J. Contribution of Archaea to total prokaryotic production in the deep Atlantic Ocean. *Applied Environmental Microbiology,* 71(5): 2303-9 (2005).

Hodges, L. R., Bano, N., Hollibaugh, J. T., & Yager, P. L. Illustrating the importance of particulate organic matter to pelagic microbial abundance and community structure - An Arctic case study. *Aquatic Microbial Ecology: International Journal*, *40*(3), 217–227. doi: 10.3354/ame040217 (2005).

IPCC, 2019: Climate Change and Land: an IPCC special report on climate change, desertification, land degradation, sustainable land management, food security, and greenhouse gas fluxes in terrestrial ecosystems [P.R. Shukla, J. Skea, E. Calvo Buendia, V. Masson-Delmotte, H.-O. Pörtner, D. C. Roberts, P. Zhai, R. Slade, S. Connors, R. van Diemen, M.

Ferrat, E. Haughey, S. Luz, S. Neogi, M. Pathak, J. Petzold, J. Portugal Pereira, P. Vyas, E. Huntley, K. Kissick, M. Belkacemi, J. Malley, (eds.)].

Ivanova, E. P., Lopez-Perez, M., Zabalos, M., Nguyen, S. H., Webb, H. K., Ryan, J., Lagutin, K., Vyssotski, M., Crawford, R. J., Rodriguez-Valera, F. Ecophysiological Diversity of a Novel Member of the Genus *Alteromonas*, and Description of *Alteromonas mediterranea* sp. nov. *Antonie van Leeuwenhoek,* Vol. 107: 119 – 132 (2014).

Kemp, P.F., Cole, J.J., Sherr, B.F., & Sherr, E.B. (Eds.). Handbook of Methods in Aquatic Microbial Ecology (1st ed.). CRC Press. https://doi.org/10.1201/9780203752746 (1993).

Kirchman, D. L., Moran, X. A. G., Ducklow, H. Microbial Growth in the Polar Oceans: Role of Temperature and Potential Impact of Climate Change. *Nature Reviews Microbiology,* Vol. 7: 451 – 459 (2009).

Kumar, A., Perlwitz, J., Eischeid, J., Quan, X., Xu, T., Zhang, T., Hoerling, M., Jha, B., Wang, W. Contribution of Sea Ice Loss to Arctic Amplification. *Advancing Earth and Space Sciences,* Vol. 37 (21) (2010).

Kwon, S., Lee, I., Park, K., Cho, K., Jung, J., Park, T., Lee, Y., Seo, S., Hahm, D. Summer net community production in the northern Chukchi Sea: Comparison between 2017 and 2020. *Frontiers in Marine Science,* Vol. 9 (2022).

Lenton, T. M. Early Warning of Climate Tipping Points. *Nature,* 1, 201 – 209 (2011).

Leu, E., Mundy, C. J., Assmy, P., Campbell, K., Gabrielsen, T. M., Gosselin, M., Juul-Pedersen, T., Gradinger, R. Arctic Spring Awakening – Steering Principles Behind the Phenology of Vernal Ice Algal Blooms. *Progress in Oceanography,* Vol. 139: 151 – 170 (2015).

López-López, A., Bartual, S.G., Stal, L., Onyshchenko, O., Rodríguez-Valera, F. Genetic analysis of housekeeping genes reveals a deep-sea ecotype of *Alteromonas macleodii* in the Mediterranean Sea. *Environmental Microbiology*, (5): 649-59 (2005).

Nansen, F. Das Bodenwasser und die Abkühlung des Meeres. *Internationale Revue der Gesamten Hydrobiologie und Hydrographie,* Nr. 1 (1912).

Nielsen, T. G., Hansen, B. W. Plankton Community Structure and Carbon Cycling on the Western Coast of Greenland During the Stratified Summer Situation. I. Hydrography, Phytoplankton and Bacterioplankton. *Aquatic Microbial Ecology,* Vol. 16: 205 – 216 (1999).

Orcutt, B.N., Sylvan, J.B., Knab, N.J., Edwards, K.J. Microbial Ecology of the Dark Ccean Above, At, and Below the Seafloor. *Microbiol Mol Biol*., 75 (2): 361 - 422 (2011).

Pontiller, B., Martinez-Garcia, S., Lundin, D., Pinhassi, J. Labile Dissolved Organic Compound Characteristics Select for Divergence in Marine Bacterial Activity and Transcription. *Frontiers in Microbiology,* Vol. 11 (2020).

Reinthaler, T., van Aken, H. M., Herndl, G. J. Major contribution of autotrophy to microbial carbon cycling in the deep Nort Atlantic´s interior. *Deep Sea Research Part II: Topical Studies in Oceanography,* Vol. 57 (16): 1572 – 1580 (2010).

Rysgaard, S., Boone, W., Carslon, D., Sejr, M., K., Bendtsen, J., Juul-Pedersen, T., Lund, H., Meire, L., Mortensen, J. An updated view on the Water Masses on the pan-West Greenland Continental Shelf and Their Link to Proglacial Fjords. *Journal of Geophysical Research, Oceans: 125* (2020).

Schauberger, C., Middelboe, M., Larsen, M., Peoples, L. M., Bartlett, D. H., Kirpekar, F., Rowden, A. A., Wenzhöfer, F., Thamdrup, B., Glud, R. N. Spatial Variability of Prokaryotic and Viral Abundances in the Kermadec and Atacama Trench regions. *Limnology and Oceanography,* Vol. 66 (6): 2095 – 2109 (2021).

Sherwood, P. B., Sosa, O., Nelson, C. E., Repeta, D., DeLong, E. Lability of High Molecular Weight Dissolved Organic Matter Polysaccharides Increases with Mild Acid or Base Treatment. *American Geophysical Union,* Ocean Science Meeting (2016).

Staroscik, A. M., Smith, D. C. Seasonal Patterns in Bacterioplankton Abundance and Production in Narragansett Bay, Rhode Island, USA. *Aquatic Microbial Ecology*, Vol. 35: 275 – 282, (2004).

Swan, B. K. *et al.* Potential for Chemolithoautotrophy Among Ubiquitous Bacteria Lineages in the Dark Ocean. *Science*, 333,1296-1300 (2011).

Topisirović, Lj., Fira, Đ., Lozo, J. Dinamička Biohemija. *Univerzitet u Beogradu Biološki Fakultet,* 2. izdanje (2016).

Volk, T., and Hoffert, M. I. Ocean Carbon Pumps: Analysis of Relative Strengths and Efficiencies in Ocean-Driven Atmospheric CO_2 Changes. *Advancing Earth and Space Sciences,* Vol. 32: 99 - 110 (1985).

Wassman, P. Arctic Marine Ecosystems an Era of Rapid Change. *Progress in Oceanography,* 90(1): 1 – 17 (2011).

Werkman, C.H., and Wood, H.G. Heterotrophic assimilation of carbon dioxide. *Advances in Enzymology and Related Areas of Molecular Biology (Nord, F.F. and Werkman, C.H., eds.),* 2, 135 – 182 (1942).

Whitman W. B., Coleman D. C., Wiebe W. J. Prokaryotes: The Unseen Majority. *Proc. Natl. Acad. Sci. U. S. A.* Vol. 95: 6578 – 6583 (1998).

Wolfer, J. Microbial Community Composition and Amino Acid Distribution in Coastal Waters off West Greenland. (2023).

Appendix

Zusammenfassung

Der Arktische Ozean ist derzeit die Region, die am stärksten vom globalen Klimawandel betroffen ist. Folglich könnten der Rückgang des arktischen Meereises und die allgemeine Erwärmung der arktischen Gewässer zu erheblichen Veränderungen in der Organismen und Ökosystemfunktion des Arktischen Ozeans führen. Einer der wichtigsten Treiber der biogeochemischen Kreisläufe im Ozean sind Mikroben. Wir haben die Dynamik der marinen heterotrophen und autotrophen mikrobiellen Gemeinschaft in den Gewässern vor Westgrönland, insbesondere von *Alteromonas,* untersucht. Die Gattung Alteromonas ist ein gramnegatives, heterotrophes Bakterium mit kosmopolitischer Verbreitung. In dieser Arbeit wurde ein besonderer Schwerpunkt auf den Beitrag zum anaplerotischen Stoffwechsel gelegt, d. h. auf die Nutzung von gelöstem anorganischem Kohlenstoff (DIC) für die Biomasseproduktion. Mithilfe der Mikroautoradiographie in Kombination mit der katalysierten Reporterablagerungs-Fluoreszenz-in-situ-Hybridisierung (CARD – FISH) haben wir die Häufigkeit, heterotrophe und chemolithoautotrophe oder anaplerotische Aktivität der Prokaryoten und Alteromonas in der Sommersaison in den Gewässern vor der Küste Westgrönlands bestimmt. Wir fanden eine tiefenabhängige Verteilung von Alteromonas mit hoher Abundanz in der photischen Zone und in küstennahen Stationen. Darüber hinaus wurde das höchste Verhältnis von Hetetrotrophie zu Chemolithoautotrophie in der photischen Zone bestimmt, wobei das niedrigste Verhältnis (< 1) in bodennahen Wasserschichten verzeichnet wurde. Alteromonas trug 7,4 % zur gesamten prokaryotischen DIC-Fixierung und 4,4 % zur prokaryotischen heterotrophen Aktivität bei. Daraus schließen wir, dass Alteromonas eine wichtige Rolle im Kohlenstoffkreislauf im Arktischen Ozean spielt.